BULLETIN OF THE GEOLOGICAL SOCIETY OF AMERICA
VOL. 66. PP. 1275-1314. 1955

EXPERIMENTAL STUDY OF THE STRENGTH OF ROCKS

By Eugene C. Robertson

4000 kg/cm²

Paper No. 136
Published under the auspices of the Committee on Experimental Geology and Geophysics and the Division of Geological Science at Harvard University.

PUBLISHED BY THE SOCIETY
OCTOBER, 1955

Made in the United States of America

BULLETIN OF THE GEOLOGICAL SOCIETY OF AMERICA
VOL. 66, PP. 1275-1314, 25 FIGS., 4 PLS. OCTOBER 1955

EXPERIMENTAL STUDY OF THE STRENGTH OF ROCKS

BY EUGENE C. ROBERTSON

ABSTRACT

An experimental investigation of the homogeneous Solenhofen limestone and a number of other rocks was made to determine their their strengths while under moderate hydrostatic pressure at room temperature. The other rocks were fossiliferous limestone, shaly limestone, marble, granite, diabase quartzite, slate, soapstone, verde antique, and sandstone. The minerals tested were pyrite, quartz, microcline, and fluorite.

Three types of experimental procedures were used: compression of solid cylinders, crushing of hollow cylinders, and punching of disks. The specimens were all carefully shaped right circular cylinders, and during the tests were jacketed to prevent penetration by the pressure fluid. The hydrostatic pressures ranged from 1 atmosphere to 4000 kg/cm^2. Measurements were made to obtain strains and stresses developed in each specimen for deformation to the point of rupture or into the plastic range; the duration of the tests was 1–8 hours.

All rock specimens exhibited a range of elastic linearity of stress with strain. Under moderate hydrostatic pressures, the limestones and marbles could be made to flow plastically to large deformations, and some heating experiments on limestone demonstrated an increase of plasticity with heating. None of the silicate rocks and minerals exhibited any plastic behavior.

The experimental data were examined with reference to various criteria of failure. The maximum shear-stress criterion was found to be reliable in predicting the yield point for the limestones, and was found to be an approximate guide to failure of limestone by rupture.

The silicate rocks failed by rupture, and their rupture strength was increased by hydrostatic pressure. A rough, empirical criterion of failure was found for rupture of silicate rocks, namely, linearity of maximum shear stress with mean stress.

CONTENTS

TEXT

ILLUSTRATIONS

TABLES

Introduction

This laboratory investigation was conducted to find some predictable regularity in the strength of fresh-rock specimens deformed to failure by fracture or plastic flow under hydrostatic pressures up to 4000 kg/cm^2, at room temperature, under pressures applied slowly and with no change of the chemical environment. Primarily, experiments were performed to examine the influence of the stress magnitude and orientation on strength, but exploratory work was also done to find the dependence of strength on stress rate and stress history, on heat, and on the type and physical character of the rocks.

F. D. Adams (1901; 1910; 1912; 1917) previously utilized the restraint of tightly fitted steel jackets to provide lateral pressure on specimens of many types of rocks. Karman (1911) and Boeker (1915) each studied the deformation of marble under hydrostatic pressure in various stress systems. Bridgman (1918; 1936; 1939; and miscellaneous data in numerous papers) has studied the strengths of rocks under low to very high hydrostatic pressure, principally by compression and shearing tests. Griggs (1936; 1939; 1940; Griggs *et al.*, 1951; 1953) is the principal modern worker in the study of rock deformation, especially of carbonate rocks and minerals. Balsley (1941) studied the strength of marble

by extension tests. Goguel (1943, Part II) has given a fairly complete analysis of the available experimental data, adding some work of his own. Handin (1953; Handin and Higgs, 1954) has given a review of recent literature and has begun a thorough study of deformation of dolomite. Joffe (1928) investigated the deformation of sodium chloride carefully.

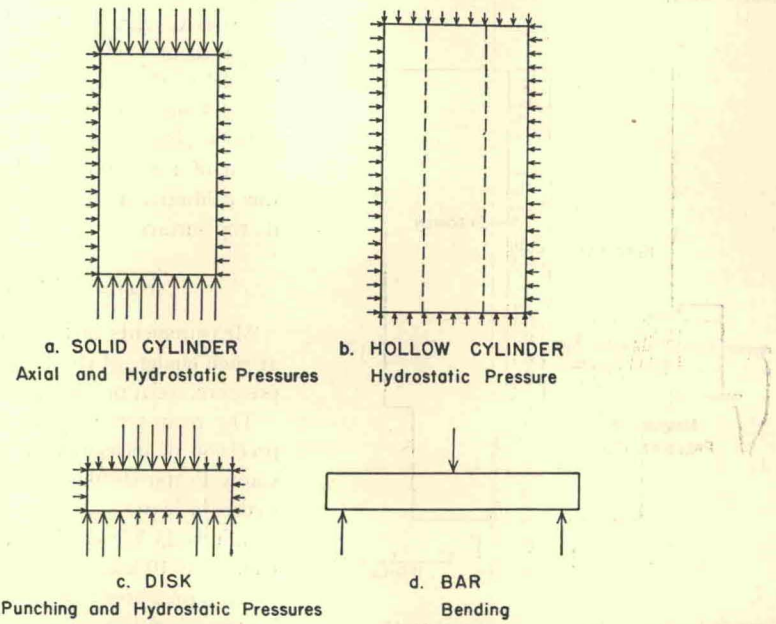

FIGURE 1.—DIAGRAMS OF THE EXTERNAL PRESSURES ON ROCK SPECIMENS IN FOUR EXPERIMENTAL PROCEDURES

In the experiments performed in this study, no tensional forces were applied; the forces were all compressive. Therefore, to avoid complication with signs of terms, the compressive stresses will be given as positive rather than negative.

The following are useful approximations:

1 ksc (kg/cm²) ≅ 1 atmos ≅ 1 bar ≅ 15 psi (lb/in²)
≅ 1 ton/ft²
1 mile depth ≅ 400 atmos
1 km depth ≅ 250 atmos

ACKNOWLEDGMENTS

Professor Francis Birch at Harvard University suggested to me the problem of finding an applicable criterion for failure in rocks, and he outlined the general and specific procedure involved in the solution of the problem. I acknowledge very gratefully Professor Birch's continued help and encouragement. The skillful machine work of Harold J. Ames with the help of L. Hammer and R. Hopewell was essential to the continuance of the investigation. Finally, I am indebted to the following men who have helped in various ways: R. K. Blumberg, P. H. Chang, C. Frondel, D. T. Griggs, H. E. McKinstry and E. Orowan.

EXPERIMENTAL RESULTS FOR LIMESTONES AND MARBLES

General Testing Procedure

Stress differences were developed within the specimens by applying hydrostatic pressure plus other loading on the external surfaces of the rock and mineral specimens. In each experiment, the difference between the stresses was increased until failure occurred. "Failure" signifies loss of strength both by breaking and by yielding. "Strength" is defined in Webster's New International Dictionary as "the quality of bodies by which they endure the application of force without breaking or yielding". In this

paper, rupture strength is the maximum stress difference at failure by breaking, and yield strength is the maximum stress difference at failure by yielding, assumed to occur at the elastic limit.

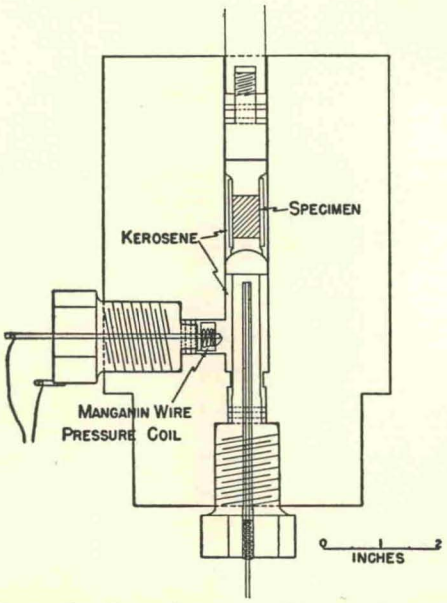

FIGURE 2.—CROSS SECTION OF TESTING CYLINDER

In one series of tests, solid cylinders of rock were compressed by hydrostatic pressure plus loading parallel to the cylinder axis (Fig. 1a). Another series of tests was made on hollow cylinders with closed ends; they were subjected only to hydrostatic pressure at the outside surfaces (Fig. 1b). Some punching experiments on disks of limestone under hydrostatic pressures were performed also (Fig. 1c). Only a few bending tests (Fig. 1d) at one atmosphere were performed. In almost all tests, the rate of loading was slow, at a rate of strain less than 1 per cent per half hour; and the length of the tests was from 1–8 hours.

A cross section of the steel testing cylinder used in most of the experiments is shown in Figure 2. The construction and use of high-pressure apparatus has been given in detail by Bridgman (for example, 1931, p. 30–77).

Hydrostatic pressure was built up in the pressure fluid in the testing chamber by advances of the piston driven by a hydraulic ram. The chamber was sealed against leaking at all openings by use of the Bridgman unsupported-area packing technique. The hydrostatic pressure was measured by balancing the change in the resistance of the manganin wire coil in the testing cylinder on a Carey-Foster bridge.

A device eliminating friction corrections in the measurement of the compressive force parallel to the axis of the steel testing cylinder was designed by Prof. Francis Birch; it is the bottom plug shown in Figure 2. The elastic strain of the hollow steel column of the plug was calibrated to give the compressive load on its top surface.

Accuracy of Measurements

Measurements in four categories were made at each change of conditions: time, hydrostatic pressure, axial pressure, and strain.

The room-temperature changes affected the precision of measurement of resistance by the Carey-Foster bridge so that the values of hydrostatic pressure were accurate only to plus or minus 25 ksc (kg/cm^2), although the sensitivity was 10 ksc.

Axial pressures measured by the strain of the bottom plug were accurate to plus or minus 50 ksc.

Rather uncertain corrections for strains in the packing and in the steel members to the measurements of shortening of solid cylinders and of punch penetration of disks reduced the accuracy of strains of the rock and mineral specimens considerably. The corrected total strain in the specimen was accurate only to within 10–20 per cent of its value, which precludes accurate computation of elastic constants; however, the reliability of the slope changes of the stress-strain curves was quite adequate for strength determinations. Longitudinal strains only were measured during the experiments; correction to the compressive stress was made for strains larger than a few per cent.

Each specimen was turned or ground to have a difference in diameter at all sections of less than 0.001 inch. The ends of the specimens were carefully ground to be perpendicular to the axes of the cylinders.

The well-known lack of homogeneity in rocks, and the anisotropy of minerals are complications in any study of their elastic properties,

although a statistical isotropy and homogeneity is approached in many fine-grained rocks, such as the lithographic limestone from Solenhofen, Bavaria, which was used for a majority of the tests. Solenhofen limestone has an extremely fine grain size (0.0002 inch), and a nearly random grain orientation is suggested by X-ray and physical-property tests.

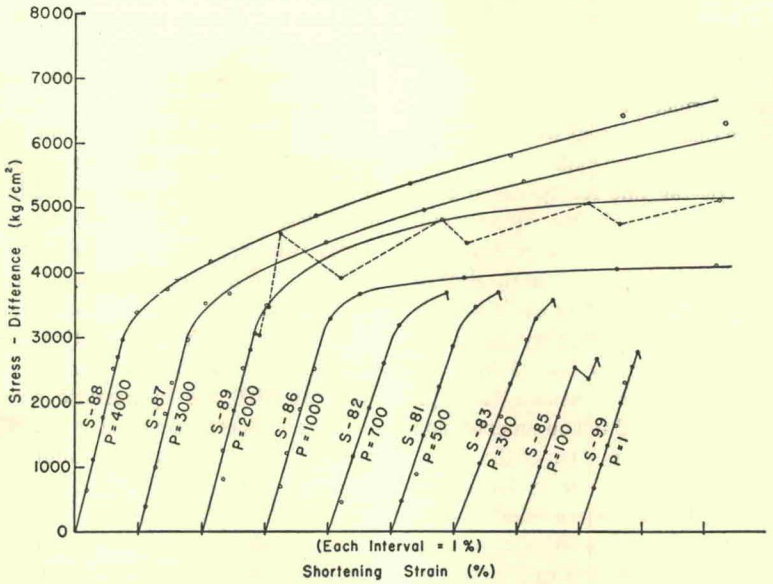

FIGURE 3.—STRESS-STRAIN CURVES FROM AXIAL-COMPRESSION EXPERIMENTS ON SOLID CYLINDERS OF SOLENHOFEN LIMESTONE

Each curve starts at zero strain; P = hydrostatic pressure in kg/cm.²

Compression of Solid Cylinders

The solid cylinders of rocks were all made ½ inch in diameter, and were ¾–1¼ inches long. Each specimen was mounted between two steel end plugs, and was jacketed with rubber tubing. Most of the experiments were done with solid end plugs (Pl. 1, fig. 2), which may have introduced certain irregularities in the stress distribution in the specimens, but the deformed specimens were quite symmetrical in appearance and consistent in strength. No lubrication was used between the steel end plugs and the specimen.

The advancing piston compressed excess of kerosene so that at contact with the end of the specimen the piston built up a hydrostatic pressure around the specimen. Thereafter, the piston produced both the hydrostatic and the differential axial pressures. A bleeder valve was used to remove kerosene, in order to maintain a constant hydrostatic pressure as the piston was advanced against the specimen. The piston was advanced intermittently, at about 5-minute intervals, each time increasing the stress difference about 200 ksc (kg/cm²), an average strain rate of about 0.02 per cent per minute in the elastic range. Testing was continued on each specimen well into the plastic range or to the rupture point.

Results from Solid-Cylinder Compression Tests on Solenhofen Limestone

The per cent decrease in length of the solid-cylinder specimens versus stress difference (total axial pressure minus hydrostatic pressure) in the cylinders are plotted in Figure 3. Within the limits of observation, the lower portion of all the curves is straight, and this justifies the application of Hooke's Law and elasticity theory to deformation below the elastic limit.

Specimens tested under hydrostatic pressures less than 1000 ksc show the abrupt termination of a rupture failure with a preceding, small

plastic flow. Specimen S-81 was shortened about 50 per cent and was considerably fractured, but nevertheless the interlocking fragments supported a compressive load greater than 1500 ksc for most of the deformation after the initial failure at 3740 ksc (Pl. 1, fig. 13). The four curves at the left in Figure 3 show considerable plastic deformation beyond the elastic limit. All specimens deformed plastically to a permanent set of more than 1 per cent were decreased slightly in density. (*See* Appendix 2.)

The dashed, zig-zag line for specimen S-89 is drawn to show how all the stress-strain curves (in solid lines in Fig. 3) were drawn in the plastic range. The peak points on the dashed line are stress-strain values after each increase of compressive stress, and the valley points are values after relaxation for at least 5 minutes. The solid line connects peak points. The high peak for S-89, which would fall on an extension of the elastic, straight-line portion of the curve, represents the stress-strain point achieved by applying additional compression suddenly, in about one second—almost an impact loading. This suggests that the limestone can withstand elastically an impact load much larger than the previously determined elastic limit. Metals also exhibit a higher elastic limit under impact loads. In the plastic range, the positions of the curves are strongly affected by the rate of application of stress, and the positions as plotted could be made to move upward considerably or downward slightly as the rate increases or decreases.

Rupture of limestone at low hydrostatic pressures seems to occur by a wedging action, (Pl. 1, figs. 7, 9), possibly formed by two sets of coalesced axial-radial and tangential-axial shears (Fig. 8c, a). (*See* Griggs, 1936, p. 552.)

The use of a jacket to prevent access of the pressure fluid into the pores of the specimen is very important in such testing as this. To confirm the difference in behavior, a test was made at 2700 ksc hydrostatic pressure of a cylinder of limestone with slots cut in its rubber jacket; the resulting rupture failure is shown in Figure 12 of Plate 1. Griggs (1936, p. 566–567) also found that penetration by the kerosene pressure fluid seems to weaken the limestone markedly beyond the elastic limit.

PLATE 1.—SOLID CYLINDERS OF SOLENHOFEN LIMESTONE

(Length of the scale bar is 1 cm.)

FIGURE 1.—SOLID-CYLINDER SPECIMEN ASSEMBLY WITH JACKET OF RUBBER TUBING AT TOP

FIGURE 2.—SOLID-CYLINDER SPECIMEN ASSEMBLY WITH SOLID END PLUGS

FIGURE 3.—S-SHAPE BUCKLING PRODUCED BY NONAXIAL LOADING

Spec. S-54; P_H = 1700 ksc; average shortening = 7.3%. $(\sigma_D)_{El\ Lim}$ = 3100 ksc.

FIGURE 4.—TENSION SIDE OF A BUCKLED SPECIMEN

(A piece of rubber is caught in a tension crack.) Spec. S-82; P_H = 700 ksc; average shortening = 12.0%; $(\sigma_D)_{Rup}$ = 3730 ksc.

FIGURE 5.—TANGENTIAL-AXIAL SHEAR LINES ON BULGED SURFACE

Spec. S-60; P_H = 500 ksc; permanent shortening = 3.5%; $(\sigma_D)_{Rup}$ = 3620 ksc.

FIGURE 6.—RUPTURE ALONG COALESCED TANGENTIAL-AXIAL SHEAR SURFACES

Spec. S-53; P_H = 170 ksc; rupture pressure uncertain.

FIGURE 7.—SPLITTING ACTION OF WEDGE IN BRITTLE RUPTURE

Spec. S-83; P_H = 300 ksc; shortening = 13%; $(\sigma_D)_{Rup}$ = 3610 ksc.

FIGURE 8.—DISPLACEMENT OF SKIN OF CYLINDER ALONG A TANGENTIAL-AXIAL SHEAR SURFACE

Spec. S-86; P_H = 1000 ksc; shortening = 16.3%; $(\sigma_D)_{El\ Lim}$ = 3100 ksc.

FIGURE 9.—WEDGE FAILURE IN BRITTLE RUPTURE

Spec. S-84; P_H = 300 ksc; shortening = 4%; $(\sigma_D)_{Rup}$ = 3600 ksc.

FIGURE 10.—PLASTICALLY DEFORMED SPECIMEN CHIPPED IN PREPARING IT FOR A SECOND TEST

Spec. S-88; P_H = 4000 ksc; shortening = 17.2%; $(\sigma_D)_{El\ Lim}$ = 2950 ksc.

FIGURE 11.—SIZE BEFORE DEFORMATION AND SIZE AFTER LARGE STRAIN INTO PLASTIC RANGE

Spec. S-89; P_H = 2000 ksc; shortening = 27.0%; $(\sigma_D)_{EL\ Lim}$ = 3100 ksc.

FIGURE 12.—RUPTURE OCCURRED BECAUSE SLOTS WERE CUT IN THE RUBBER JACKET TO PERMIT ACCESS OF KEROSENE PRESSURE FLUID

Spec. S-93; P_H = 2700 ksc; $(\sigma_D)_{Rup}$ = 3080 ksc.

FIGURE 13.—CYLINDER AFTER GREAT DEFORMATION AT A LOW CONFINING PRESSURE

Spec. S-81; P_H = 500 ksc; shortening = 53%; $(\sigma_D)_{Rup}$ = 3740 ksc.

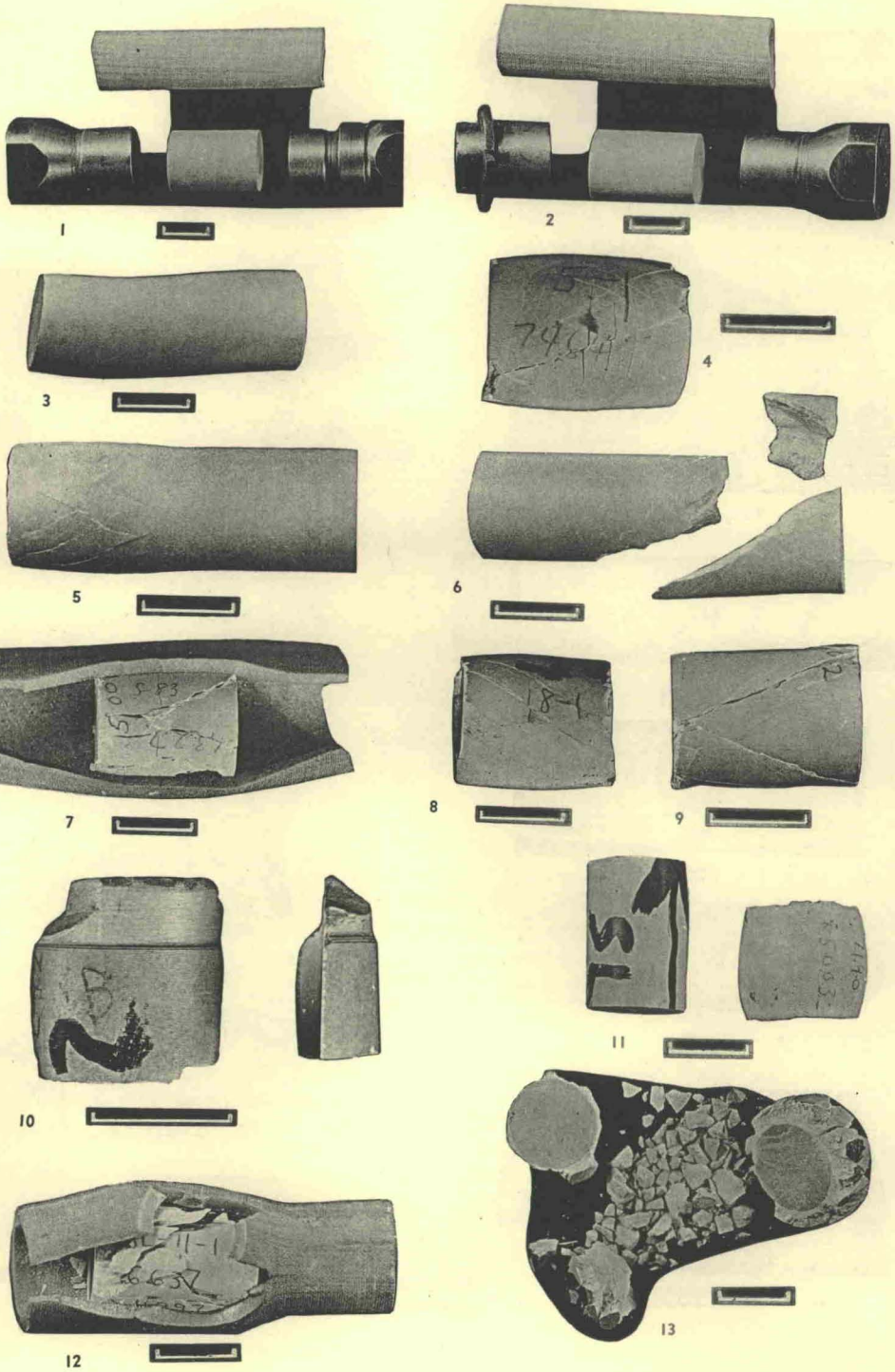

SOLID CYLINDERS OF SOLENHOFEN LIMESTONE

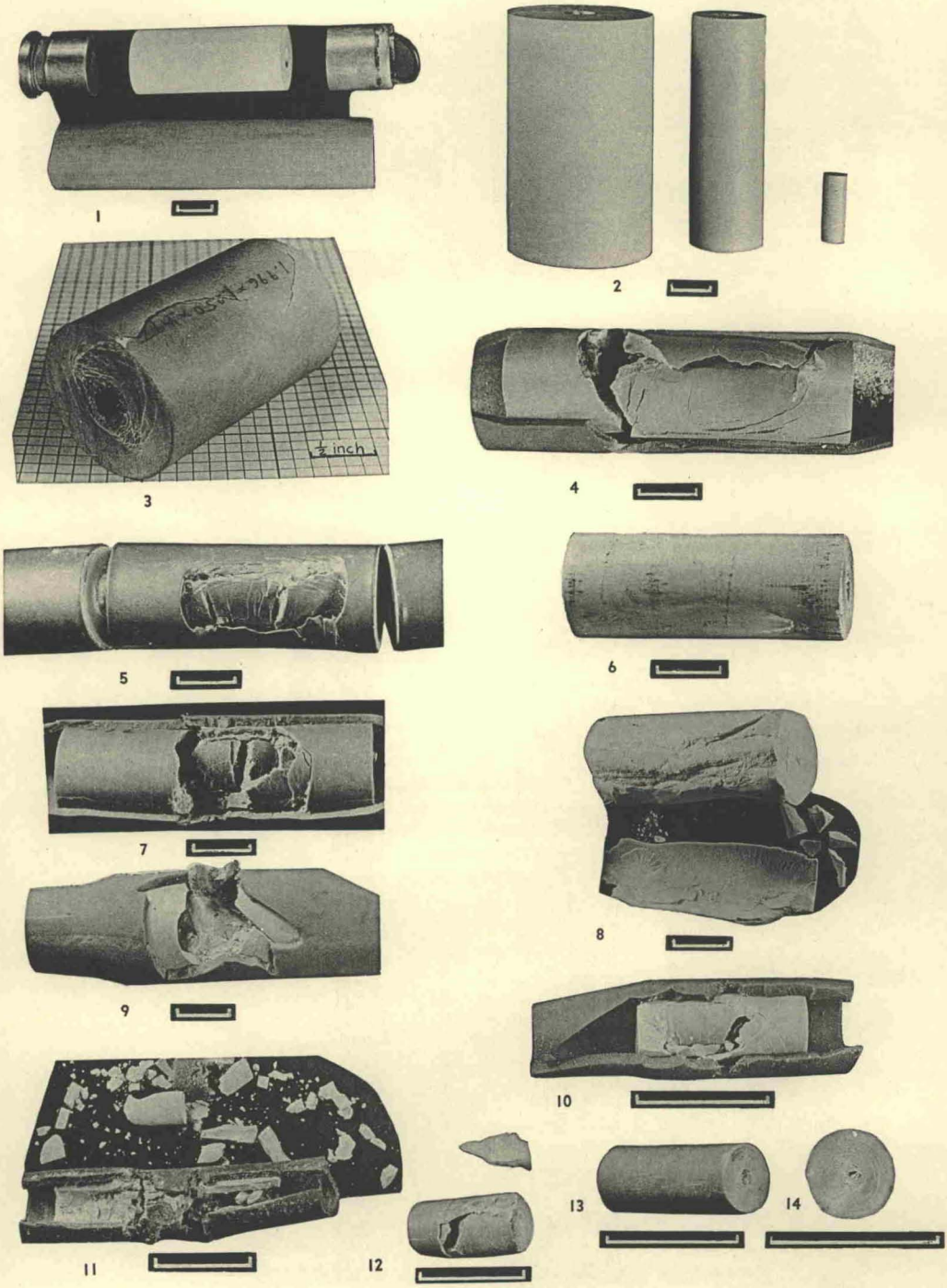

HOLLOW CYLINDERS OF SOLENHOFEN LIMESTONE

Results from Cyclic Compression Tests on Solid Cylinders of Solenhofen Limestone

In metals testing, the raising of the elastic limit (*i.e.*, raising the yield strength) by successive and increasing deformations of the piece into the plastic range is called strain hardening or work hardening. The metal is actually hardened by this processing, as well as strengthened. In testing limestone, a similar raising of the elastic limit was found, although there was no observable hardening of the limestone. It is suggested that the term, strain strengthening, may be more appropriate for this phenomenon in rocks, and it will be so used in this paper.

The limestone is strengthened (Fig. 4) while in the plastic condition, but within 24 hours after unloading loses its added yield strength, in contrast to the behavior of metals. By repeatedly loading and unloading solid cylinder S-128 (while under hydrostatic pressure during and between cycles) the yield strength was raised from 2800 ksc to 5100 ksc. (The total residual strain was 7 per cent.) Similar curves are given for S-124. The temporary nature of the strain strengthening is indicated by the fact that the elastic limits of the specimens when tested 24 hours and 64 days after removal from the press had both dropped back to 3100 ksc, although the succeeding plastic parts of the curves are steeper than in the first cycle.

Several other tests not shown in Figure 4 were made, which are relevant. The strength of a solid cylinder previously shortened 4 per cent and presumably strain strengthened under hydrostatic pressure was tested several months later at 1 atm, and its rupture strength was found to be much reduced; 1900 ksc instead of the usual 2800 ksc. Another cylinder, tested wholly in air, was loaded once to a stress of 1500 ksc, unloaded, and immediately reloaded to rupture failure; some plastic yielding

---

PLATE 2.—HOLLOW CYLINDERS OF SOLENHOFEN LIMESTONE

(Length of the scale bar is 1 cm.)

FIGURE 1.—HOLLOW-CYLINDER SPECIMEN ASSEMBLY WITH RUBBER JACKET BELOW

FIGURE 2.—THREE SIZES OF HOLLOW CYLINDERS TESTED, WITH OUTSIDE DIAMETERS: 1¼ INCHES, ⅝ INCHES AND 3/16 INCHES

FIGURE 3.—DIAGONAL VIEW OF A 1¼-INCH MEDIUM-WALLED CYLINDER

The hole was two-thirds full of clay to prevent complete collapse; spec. S-45; $\alpha = 2.52/1$; $(P_H)_{Rup} = 2400$ ksc.

FIGURE 4.—RUPTURE OF MEDIUM-WALLED CYLINDER ON A CURVED TANGENTIAL-RADIAL SHEAR SURFACE AT THE TOP AND HINGED ALONG THE BOTTOM

Spec. S-36; ⅝-in. dia.; $\alpha = 2.70/1$; $(P_H)_{Rup} = 2350$ ksc.

FIGURE 5.—RUPTURE FAILURE OF COPPER-JACKETED SPECIMEN

Spec. S-9; ⅝-in. dia.; $\alpha = 2.50/1$; $(P_H)_{Rup} = 1980$ ksc.

FIGURE 6.—PLASTIC FLOW OF A THICK-WALLED SPECIMEN

Spec. S-13; ⅝-in. dia.; $\alpha = 5.0/1$; $(P_H)_{Max} = 4500$ ksc.

FIGURE 7.—BRITTLE COLLAPSE OF A THIN-WALLED SPECIMEN

Spec. S-32; ⅝-in. dia.; $\alpha = 1.56/1$; $(P_H)_{Rup} = 1430$ ksc.

FIGURE 8.—EXFOLIATION OF HIGHLY DEFORMED CYLINDER

Spec. S-12; ⅝-in. dia.; $\alpha = 3.33/1$; $(P_H)_{Rup} = 3280$ ksc.

FIGURE 9.—RUPTURE OF CYLINDER CUT IN HALF ON A PLANE AT 45° WITH THE AXIS

Spec. S-70; ⅝-in. dia.; $\alpha = 2.56/1$; $(P_H)_{Rup} = 2310$ ksc.

FIGURE 10.—RUPTURE OF A SMALL MEDIUM-WALLED SPECIMEN

Spec. S-108; 3/16-in. dia.; $\alpha = 2.44/1$; $(P_H)_{Rup} = 3100$ ksc.

FIGURE 11.—BRITTLE FAILURE OF A SMALL THIN-WALLED CYLINDER

Spec. S-21; 3/16-in. dia.; $\alpha = 1.78/1$; $(P_H)_{Rup} = 1670$ ksc.

FIGURE 12.—RUPTURE OF A SMALL MEDIUM-WALLED CYLINDER

Spec. S-20; 3/16-in. dia.; $\alpha = 2.50/1$; $(P_H)_{Rup} = 3140$ ksc.

FIGURE 13.—SPALLING IN HOLE AND ELLIPTICAL CROSS SECTION AFTER FAILURE

Spec. S-64; 3/16-in. dia.; $\alpha = 3.61/1$; $(P_H)_{Max} = 5420$ ksc.

FIGURE 14.—SPALLING AND PLASTIC FLOW IN A THICK WALLED CYLINDER

Spec. S-109; 3/16-in. dia.; $\alpha = 3.57/1$; $(P_H)_{Max} = 4000$ ksc.

preceded the rupture, which occurred at 3100 ksc instead of 2800 ksc.

Two other cylinders were compressed into the plastic range, and while retaining the axial loads, the confining hydrostatic pressure on them was rapidly lowered from 3000 ksc to zero. Both cylinders ruptured at a stress difference of about 4300 ksc, while the falling hydrostatic pressure was still between 1000 and 2000 ksc. This high strength may be due in part to impact loading as well as to strain strengthening.

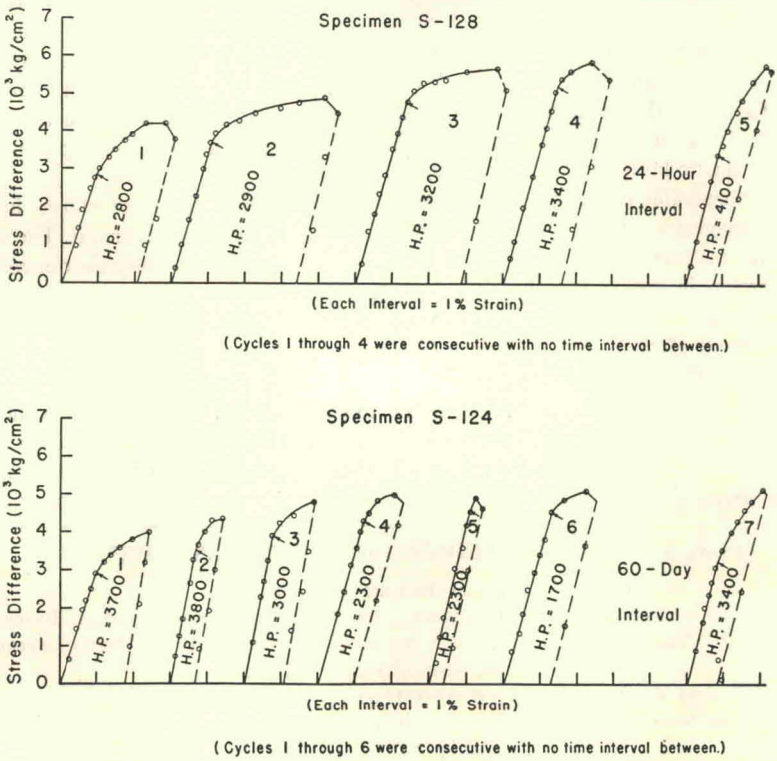

FIGURE 4.—CYCLIC-COMPRESSION EXPERIMENTS ON SOLID CYLINDERS OF SOLENHOFEN LIMESTONE

Considerable work needs to be done to evaluate the effects of cyclic testing (including the Bauschinger effect) and of the loading rate on the yield and rupture strengths of limestone. The qualitative work reported here indicates the variety and complexity of the results from such testing.

Results from Solid-Cylinder Compression Tests On Other Limestones and Marbles

The stress-strain curves of Figure 5 show the strengths at various hydrostatic pressures of various limestones and marbles. (*See* Appendix 1 for descriptions of carbonate rocks.) Most of the specimens of each rock were cut perpendicular to the foliation of the original block of rock; therefore, the strengths of the specimens cannot be considered as averages for the rocks, because both yield and rupture strengths differ in a foliated rock. As an example of the importance of foliation on strength, Griggs *et al.* (1951, Fig. 3) found a difference of 350 per cent in the yield strength in extension between two specimens of Yule marble oriented at 90° to each other with respect to the foliation.

The two marbles were considerably weaker than Solenhofen limestone. The Becraft limestone exhibited more coherence than the marbles but less than the Solenhofen limestone, possibly because of its coarse grain size and large fossil relicts. The shaly impurity in the New Scotland limestone seems to increase its rupture strength and increase its brittleness over the more pure carbonate rocks.

The experiment on Wm. Henry Bay marble was performed to examine the effect of the

relatively high porosity of the marble (5 per cent) and of its very crumbly character on its deformation. Specimen WHB-1 was compressed under a hydrostatic pressure of 3000 ksc to a termined by inspecting the specimen after each test; this method introduced some uncertainty in that the pressure at failure may have been heightened by strain strengthening since it had

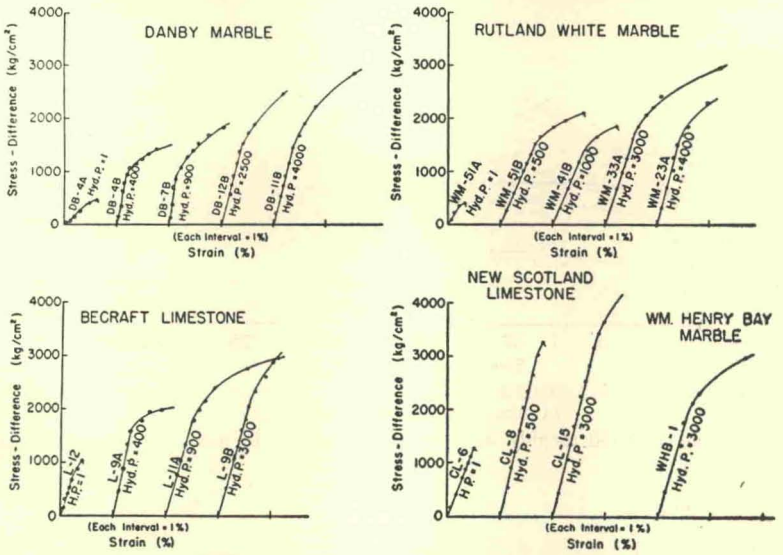

FIGURE 5.—STRESS-STRAIN CURVES FOR SOLID CYLINDERS OF VARIOUS MARBLES AND LIMESTONES
Each curve starts at zero strain; Hyd. P. = hydrostatic pressure in kg/cm².

longitudinal strain of 8 per cent at a stress difference of 5000 ksc. The density was increased in the test from 2.55 to 2.67, and the specimen was much less friable after the test.

The full extent of strain in the plastic range produced in several specimens of limestone and marble is shown in Figure 6. The curves show the large plastic deformation possible in carbonate rocks without rupture, when carried on at moderate hydrostatic pressures.

Compression of Hollow Cylinders

Most of the hollow cylinders were made with a $\frac{5}{8}$-inch outside diameter, although some additional experiments were performed on $1\frac{1}{4}$-inch and $\frac{3}{16}$-inch specimens of the Solenhofen limestone (Pl. 2). The size of the hole in the hollow cylinders was varied in each test series.

The hollow cylinders were subjected to hydrostatic pressure on the outside surface (Fig. 1b), the pressure being increased until failure occurred. The recognition of failure by rupture was by the sharp sound of the sudden collapse of the cylinder. Failure by plastic flow and spalling of thick-walled cylinders was determined by inspecting the specimen after each test; this method introduced some uncertainty in that the pressure at failure may have been heightened by strain strengthening since it had to be bracketed by tests below and then above that pressure. However, these approximate results were checked by a series of tests by a procedure in which the strain at the inside surface was measured by the change in volume of the hole. The specimen was coupled to a long hollow steel stem which protruded through the bottom plug and was connected by hose to a manometer tube. Any bubbles of air entrapped in the measuring column were removed by flushing the column at the beginning of each experiment. The major source of error was from changes in position of the specimen relative to the manometer tube because of the compression of the rubber packing around the stem, but this displacement could be corrected adequately for strength determinations.

Results from Hollow-Cylinder Tests

The curves in Figure 7 are plotted from tests on the three sizes of hollow cylinders of Solenhofen limestone at failure. The curves show the relationship of rupture strength to wall thickness (related directly to hydrostatic pressure and ratio of radii respectively). There seemed to be a dichotomy of a total collapse failure for

radius ratios less than 3.0 and spalling failure for ratios greater than 3.0. The failure by spalling was a rupturing in a thin layer at the inside surface, accompanied by plastic deformation in a middle layer and by elastic strain in the outer part of the cylinder.

Some experimental data on glass fibers (Griffith, 1920; Orowan, 1949, p. 198) indicate that fibers with very small diameters are stronger than large fibers. Griffith attempted to explain the discrepancy in strengths as due to fewer surface cracks about 2 microns long, on the smaller fibers. Recent experiments on glass (Preston, 1954) indicate that this widely accepted size effect on strength is incorrect; evidently systematic procedural errors account for the apparent difference in strength. The greater rupture strength of the small limestone

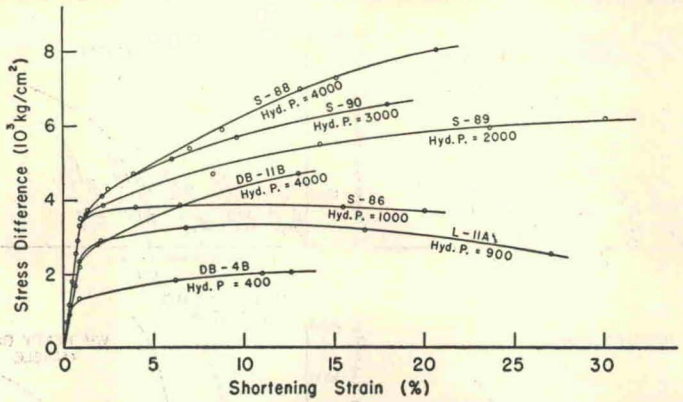

FIGURE 6.—COMPLETE STRESS-STRAIN CURVES FOR SOLID CYLINDERS OF SOLENHOFEN LIMESTONE, DANBY MARBLE, AND BECRAFT LIMESTONE

Stress difference was corrected roughly for increase in diameter by assuming no volume change with shortening.

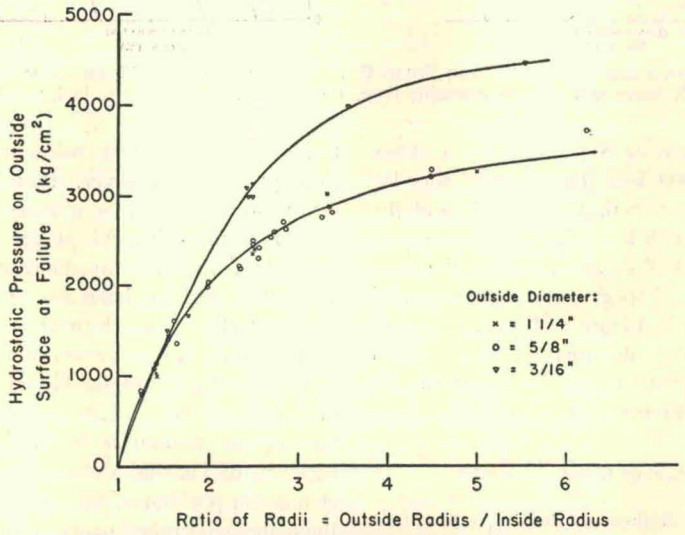

FIGURE 7.—HYDROSTATIC PRESSURE AT FAILURE VS. RATIO OF RADII FOR THREE SIZES OF HOLLOW CYLINDERS OF SOLENHOFEN LIMESTONE

There is a very close agreement between the results for the 1¼-inch cylinders and the ⅝-inch cylinders. However, the 3/16-inch cylinders are apparently much stronger than the larger specimens, although all specimens were prepared and tested under similar conditions.

cylinders may be due either to unrecognized differences in processing the cylinders or to fewer imperfections of gross dimension (e.g., bedding planes) than in the larger cylinders.

(Pl. 1, figs. 5, 8). Such helical shear lines (Lueder's lines) have been observed on solid cylinders in compression in the brittle failure of metals; to obtain this relation between the

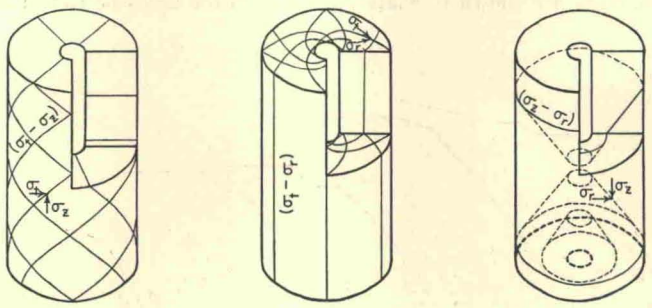

FIGURE 8.—THEORETICAL SHEARING SURFACES IN A HOLLOW CYLINDER UNDER EXTERNAL HYDROSTATIC PRESSURE
After King, 1912, Figure 1.

A comparison of the theoretical and actual modes of yield failure is of interest here. Three families of theoretical elastic shearing surfaces can develop in a hollow cylinder depending on the three possible orientations of the principal stresses (Fig. 8). The maximum, intermediate, and minimum principal stresses each may have one of three orientations in cylindrical coordinates: axial, radial, and tangential or circumferential. By elasticity theory, the maximum shear surfaces are at 45° to the directions of the maximum and the minimum principal stresses, and on each of these surfaces there acts the appropriate maximum shear stress (equal to half the difference of the maximum and minimum principal stresses in any stress system).

In my experiments, actual fracture along which rupture occurred (even in the coarse-grained igneous rocks) resembled very closely the shape of the equiangular spiral of the tangential-radial shear surface shown in Figure 8b; the failure was a hinged "trap door" collapse (Pl. 2, figs. 3, 4). The axial-radial shear surface (Fig. 8c) was also observed at the ends of the "trap door" in some of the hollow cylinders. The tangential-axial shear surface (Fig. 8a) was seen on the surfaces of some solid cylinders stresses, the tangential stress may become relatively tensile in the outer skin owing to lateral expansion as the cylinder is shortened.

In Figure 9 are stress-strain curves for some hollow cylinders. There seems to be a marked yielding at the elastic limit, although the yield points chosen are somewhat arbitrary. The four curves at the left in Figure 9 are from tests of thick-walled specimens, (Pl. 2, fig. 6); the beginning of spalling was at the first large plastic strain (horizontal line on the curve). A perceptible surging of the kerosene in the manometer column occurred at the beginning of spalling, and therefore the spalling was not a release fracturing following the release of pressure. By continued application of hydrostatic pressure on a thick-walled cylinder, it could be closed down tightly on the spalled particles inside the cylinder, usually resulting in an elliptical cross section to the cylinder.

A series of tests were performed to determine the effect of a single plane of weakness in hollow cylinders on their strength, and incidentally to evaluate the importance of friction on such planes. Five hollow cylinders were cut in half along planes at 0°, 30°, 45°, 60°, and 90° to the axes of the cylinders. No sliding was observed on the planes, and no important

departure from the average strength of cylinders of this size nor from the usual tangential-radial surface of failure was found (Pl. 2, fig. 9).

Pictures of some of the deformed 1¼-inch and 3/16-inch specimens are shown in Plate 2.

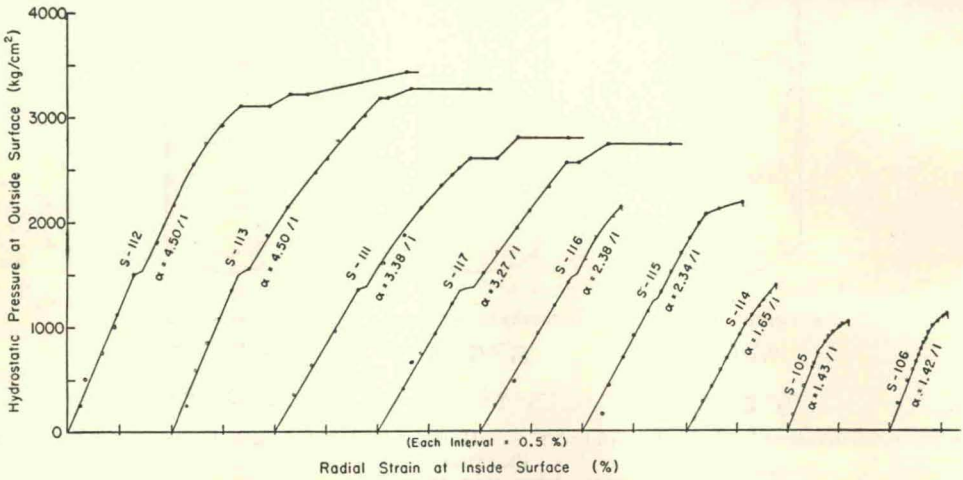

FIGURE 9.—STRESS-STRAIN CURVES FROM CRUSHING EXPERIMENTS ON HOLLOW CYLINDERS OF SOLENHOFEN LIMESTONE

Each curve starts at zero strain; α = ratio of radii = outside radius/inside radius.

The manner of failure was the same in all three sizes.

The type of material used for the jacket on the specimens did not seem to affect the strength of limestone, judging from the identical rupture strengths of copper-jacketed and rubber-jacketed hollow cylinders. However, Bridgman (1947b, p. 253) found that the "tensile" strength of glass under 25,000 ksc hydrostatic pressure was 11,000 ksc with rubber and 22,000 ksc with copper jackets.

Many experiments were done on hollow cylinders of Danby marble, Rutland white marble, Yule marble, calcite, New Scotland limestone, and Becraft limestone. Curves similar to those in Figures 7 and 9 were obtained from the data, but the results are only qualitative since the effect of rock foliation was not adequately accounted for.

Punching of Disks

The disks were all flat, solid cylinders, 5/8 inch in diameter and from 0.148 inch to 0.281 inch thick. The external pressure system is shown diagrammatically in Figure 1c, and the die and punch assembly is shown in Figure 1 of Plate 3. The diameter of the punch pin is 0.308 inch. The copper cups (at top in Pl. 3, fig. 1) were fitted over the steel pieces and were used to keep the kerosene from the disk; they were held tightly against the steel by the rubber jacket. The same instrumentation and the same method of producing hydrostatic pressure and axial loading as in the solid-cylinder tests were used.

Punching produces approximately a stress system of simple shear only. This simple stress configuration is made complex if the piece being punched is too thick, so most of the disks were made less than ¼ inch in thickness.

Solenhofen limestone was the only rock tested by punching, and the experimental data are reproduced in the curves in Figure 10. Hydrostatic pressure has a decided strengthening effect in punching tests. The pattern of rupture in the specimens shown in Figures 5 and 7 of Plate 3 consists of a circular sheared portion under the punch pin, and the radial cracks in the outer portion at about 45° or 90° intervals. For hydrostatic pressures above about 4000 ksc, the stress-strain curves for disks have elastic and plastic parts such as in the curves from solid-cylinder tests at high confining pressures. The maximum penetration of the punch in S-120 while under the maximum pressure was about 1/32 inch (Pl. 3, figs. 3, 4).

Results of Heat and Pressure Studies

A number of experiments were performed in which heat as well as pressure was applied to reconnoiter the effect of higher temperatures than 20° C on the strength of hollow cylinders of Solenhofen limestone and Yule marble. A large pressure vessel with an internal furnace was used, and the pressure fluid was nitrogen gas. The temperature was measured by a chromel-alumel thermocouple and was roughly controlled to within plus or minus 20° C. The cylinders of limestone and marble had about the same dimensions: ⅝ inch outside diameter, 1½ inches long, and ¼ inch inside diameter. The samples and steel end pieces were sealed in copper jackets.

The results of the heating experiments on hollow cylinders are listed in Table 1. The figures of the decrease in outside diameter in Table 1 were taken at the smallest diameter of the inevitably elliptical cross section which resulted from the plastic flow.

In specimens S-24 and S-10 (Pl. 3, figs. 10, 12, 13) the bore was closed down uniformly and completely for about half of the length (with a maximum 0.060-inch decrease in outside diameter), and in places the walls coalesced so well that only a trace of the hole remained. An increase in the density was found for a disk cut from the middle of S-10: the new density was 2.70, compared to the original of 2.61.

An attempt was made to cause failure in S-42 and S-43 by rupture by steadily increasing the hydrostatic pressure at constant temperature. For S-42 held at 400° C, rupture occurred at 3900 ksc after raising the pressure from 2000 ksc in a period of one hour. Specimen S-43 held at 500° C, merely closed down after raising the pressure from 2100 ksc to 5100 ksc in a period of 2 hours; the diameter of the inside hole changed from 0.26 inch to about 0.15 inch. The strength of the limestone was strikingly demonstrated by the extrusion of the low-carbon steel of the end plugs into the holes in the ends of the limestone cylinder (Pl. 3, figs. 11, 12).

The specimens may have had as much as ½ per cent water in the pores, which might have promoted plastic deformation by recrystallization, but this effect was not evaluated.

Three preliminary conclusions on the 12-hour (or longer) heating experiments can be made: the rate of plastic deformation increases with increasing temperature; at temperatures above 500° C, a pressure near or above that for rupture at 20° C will cause rapid, large plastic flow, but

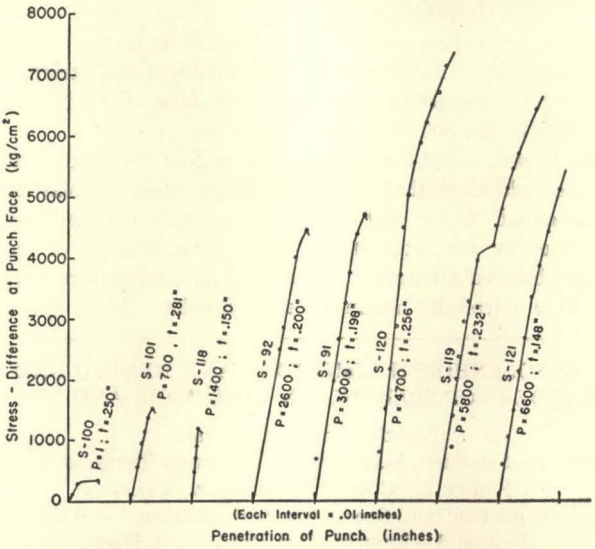

FIGURE 10.—STRESS-STRAIN CURVES FROM PUNCHING EXPERIMENTS ON DISKS OF SOLENHOFEN LIMESTONE

Each curve starts at zero penetration; P = hydrostatic pressure in kg/cm²; t = thickness of disk in inches.

without rupture; and at temperatures between 400° C and 500° C, plastic flow occurs, but rupture can be produced, although apparently only at a pressure at least 50 per cent higher than that for rupture at 20° C.

Griggs *et al.* (1951, Figs. 1, 2; 1953, Fig. 1) have recently completed a series of experiments on some oriented solid cylinders of Yule marble and single crystals of calcite deformed at room temperature, dry; at 150° C and 300° C, dry; and at 150° C and 300° C, with small amounts of water. In general, the yield strengths of the cylinders were lowered about 40 per cent by the heat and still further by the interstitial water. Although Griggs observed a lowering of the *yield* strength of Yule marble by heating, I observed a raising of the *rupture* strength of Solenhofen limestone by heating. Since concurrent strain measurements were not made in my experiments, the effect of the heat on the yield strength was not determined. At "blue heat" (about 300° C), the tensile (rupture) strength of some steel is raised 15 per cent over the strength at room temperature, although the strength falls off again as the temperature is further increased.

Separation of hydrostatic-pressure effects from heat effects on plasticity by recrystallization in Yule marble is difficult, but apparently there is an increase of recrystallization with increasing temperature (Griggs, Turner, Borg, and Sosoka, 1951, p. 1393–1394; 1953,

---

PLATE 3.—DISKS OF SOLENHOFEN LIMESTONE AND HEATED AND COMPRESSED HOLLOW CYLINDERS OF SOLENHOFEN LIMESTONE AND YULE MARBLE

(Length of scale bar is 1 cm.)

FIGURE 1.—SPECIMEN ASSEMBLY FOR PUNCHING TESTS ON DISKS

FIGURE 2.—CORE PUNCHED FROM A DISK

(The copper cups were also punched out.) Spec. S-92; P_H = 2600 ksc; t = 0.200 in.

FIGURE 3.—PUNCHED-OUT BULGE IN A DISK

Density was decreased 3.2%; spec. S-120; P_H = 4700 ksc; t = 0.256 in.

FIGURE 4.—PUNCHED DEPRESSION IN SAME DISK

Maximum penetration of punch = 0.025 in.; spec. S-120; P_H = 4700 ksc; t = 0.256 in.

FIGURE 5.—DISK TESTED IN AIR

Spec. S-100; P_H = 1 atmos.; t = 0.250 in.

FIGURE 6.—DEPRESSION PUNCHED IN A THIN DISK

Spec. S-121; P_H = 6600 ksc; t = 0.148 in.

FIGURE 7.—SPECIMEN BROKE BECAUSE OF THE WEAKENING EFFECT OF KEROSENE LEAKING PAST A COPPER CUP TO THE DISK, ALTHOUGH THE CONFINING PRESSURE WAS HIGH

Spec. S-102; P_H = 4000 ksc; t = 0.234 in.

FIGURE 8.—DEPRESSION PUNCHED IN A THICK DISK

Spec. S-119; P_H = 5800 ksc; t = 0.232 in.

FIGURE 9.—HOLLOW CYLINDER OF SOLENHOFEN LIMESTONE WHICH RUPTURED AT P_H = 3900 KSC AND T = 400° C

Test period = 1 hr.; spec. S-42; α = 2.40/1.

FIGURE 10.—HOLLOW CYLINDER OF SOLENHOFEN LIMESTONE SHOWING FLOW TOWARD THE HOLE

The end of the cylinder has been cut off where the closing down was almost complete. Spec. S-24; P_H = 2100 ksc; T = 700° C; α = 2.55/1; test period = 6 hrs.

FIGURE 11.—CLOSE-UP OF EXTRUDED STEEL PLUG AND END OF LIMESTONE CYLINDER

Spec. S-43; α = 2.40/1; $(P_H)_{Max}$ = 5100 ksc; T = 500° C; 3 test periods = 39 hrs. total.

FIGURE 12.—CROSS SECTIONS OF HOLLOW CYLINDER OF SOLENHOFEN LIMESTONE DEFORMED BY HEAT AND PRESSURE

Spec. S-10; α = 2.50/1; $(P_H)_{Max}$ = 2600 ksc; T = 600° C; test period = 3 hrs.

FIGURE 13.—CONICAL CUP, $\frac{3}{16}$ INCH ACROSS AND $\frac{1}{4}$ INCH DEEP

In end of same specimen—Spec. S-10.

FIGURE 14.—RUPTURED HOLLOW CYLINDER OF YULE MARBLE

Spec. YM-15; α = 2.38/1; $(P_H)_{Rup}$ = 1300 ksc; T = 300° C; test period = 2 hrs.

FIGURE 15.—HOLLOW CYLINDER OF YULE MARBLE FLATTENED (0.097 IN.) TO AN ELLIPTICAL CROSS SECTION

Spec. YM-14; α = 2.37/1; $(P_H)_{Max}$ = 2300 ksc; T = 400° C; test period = 20 hrs.

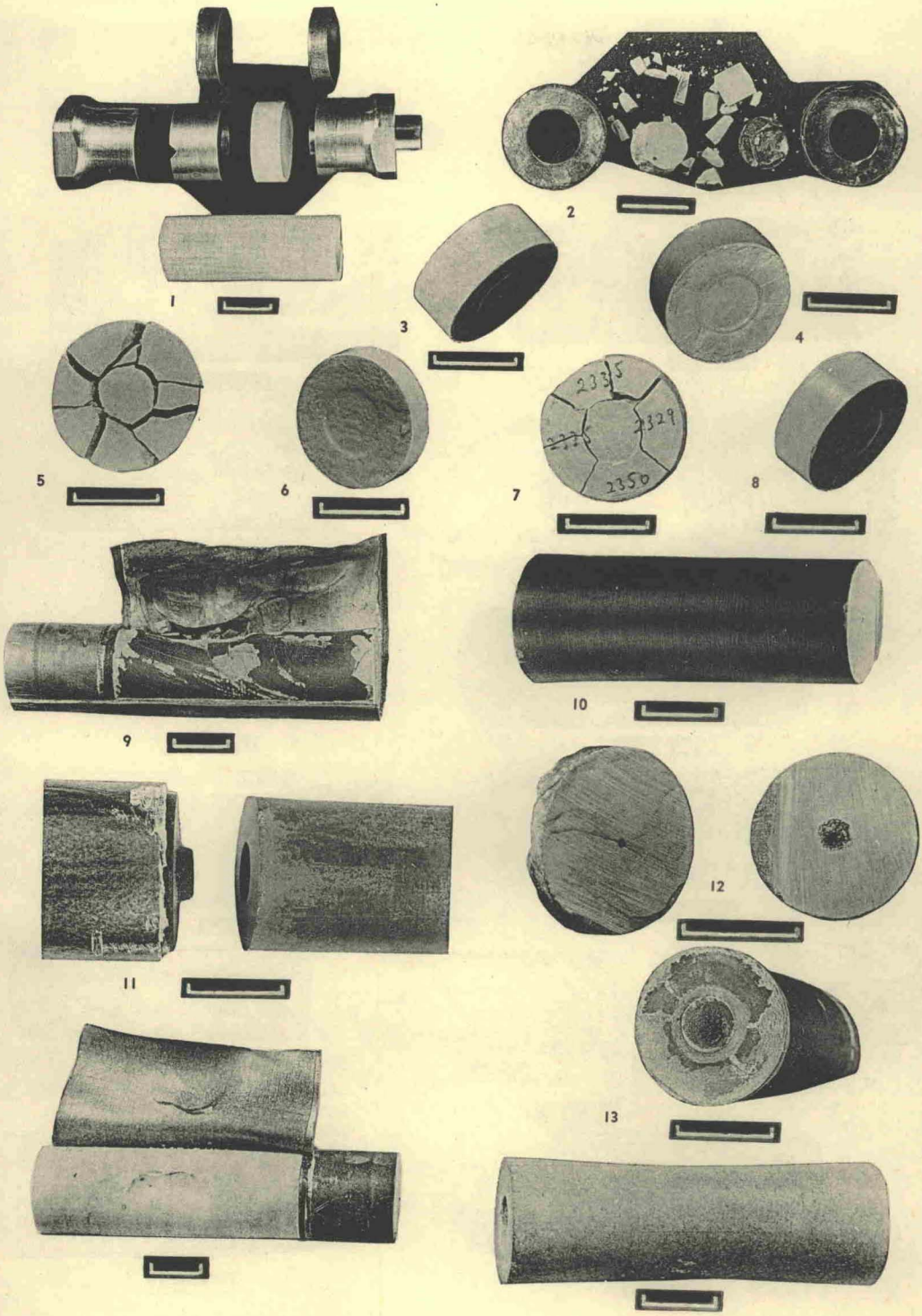

DISKS OF SOLENHOFEN LIMESTONE AND HEATED AND COMPRESSED HOLLOW CYLINDERS OF SOLENHOFEN LIMESTONE AND YULE MARBLE

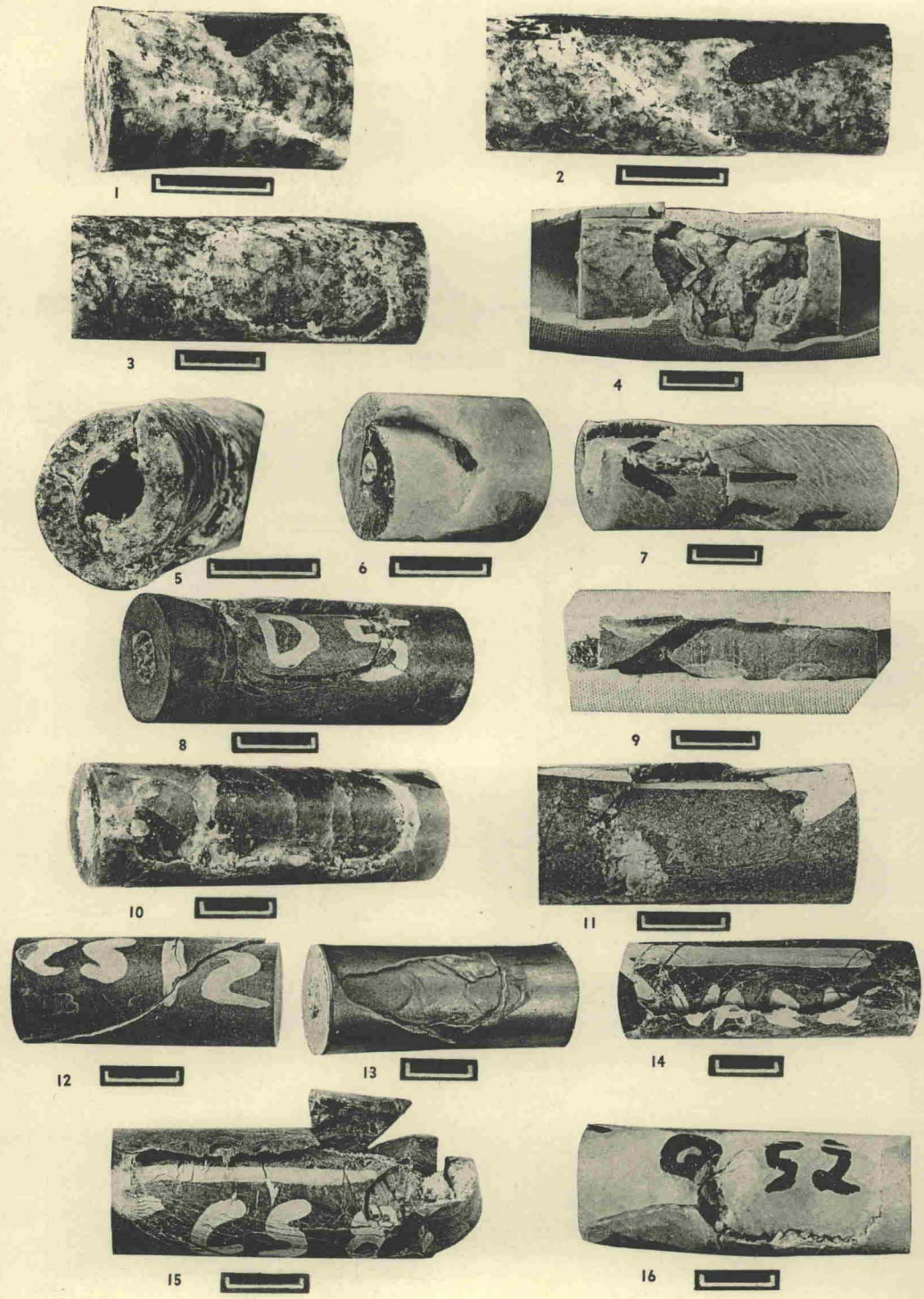

SOLID AND HOLLOW CYLINDERS OF VARIOUS SILICATE ROCKS AND MINERALS

p. 1341–1342). (Recrystallization may be characterized by healed glide and fracture planes in the marble grains.) The early heating experiments and microscope studes of Adams and Nicolson (1901) on solid cylinders of Carrara marble, support my observations that a minimum temperature of about 400° C is required to get plasticity by extensive recrystallization in short test periods. Increase of time under load and heat increases the amount of recrystallization of marble also (reported by all observers).

The possibility that the plastic flow might be aided by a polymorphic transition was considered, but it seems very unlikely. An approximate thermodynamic computation for the calcite-aragonite transformation shows that a mean pressure of about 10,000 ksc would be

---

PLATE 4.—SOLID AND HOLLOW CYLINDERS OF VARIOUS SILICATE ROCKS AND MINERALS

(Length of the scale bar is 1 cm.)

FIGURE 1.—RUPTURE ALONG A PLANAR SHEAR SURFACE OF A SOLID CYLINDER OF BARRE GRANITE
Angle with axis = 20°; spec. BG-17A; P_H = 500 ksc; $(\sigma_D)_{Rup}$ = 4350 ksc.

FIGURE 2.—RUPTURE ALONG A PLANAR SHEAR SURFACE AT 22° WITH CYLINDER AXIS IN A LONGER SPECIMEN OF BARRE GRANITE
Spec. BG-20; P_H = 550 ksc; $(\sigma_D)_{Rup}$ = 4800 ksc.

FIGURE 3.—RUPTURE ALONG "TRAP-DOOR" IN MEDIUM-WALLED HOLLOW CYLINDER OF BARRE GRANITE
Spec. BG-6; α = 3.19/1; $(P_H)_{Rup}$ = 3840 ksc.

FIGURE 4.—COLLAPSE OF THIN-WALLED HOLLOW CYLINDER OF CHELMSFORD GRANITE
Spec. C-1; α = 1.67/1; $(P_H)_{Rup}$ = 1950 ksc.

FIGURE 5.—END VIEW OF A TANGENTIAL-RADIAL SHEAR SURFACE, IN A HOLLOW CYLINDER OF BARRE GRANITE
Spec. BG-9; α = 1.90/1; $(P_H)_{Rup}$ = 2230 ksc.

FIGURE 6.—HELICAL SHEAR SURFACE IN A HOLLOW CYLINDER OF FLUORITE, CUT FROM A SINGLE CRYSTAL WITH THE AXIS PARALLEL TO AN A-AXIS
Spec. FT-15; α = 3.16/1; $(P_H)_{Rup}$ = 4450 ksc.

FIGURE 7.—RUPTURE AT THE END OF A HOLLOW CYLINDER OF MICROCLINE FELDSPAR
Spec. F-5; α = 3.18/1; $(P_H)_{Rup}$ = 3960 ksc.

FIGURE 8.—FAILURE OF A HOLLOW CYLINDER OF HOLYOKE DIABASE
Spec. D-5; α = 3.19/1; $(P_H)_{Rup}$ = 4410 ksc.

FIGURE 9.—DOUBLE-WEDGE SHEARING SURFACES (EACH AT 32° WITH AXIS) IN A SOLID CYLINDER OF PYRITE
Spec. P-2; P_H = 500 ksc; $(\sigma_D)_{Rup}$ = 5070 ksc.

FIGURE 10. "TRAP-DOOR" COLLAPSE OF A HOLLOW CYLINDER OF CHESHIRE QUARTZITE
Spec. CQ-22; α = 3.20/1; $(P_H)_{Rup}$ = 4750 ksc.

FIGURE 11.—COLLAPSE OF A HOLLOW CYLINDER OF COPPER ORE
Spec. CO-5; α = 3.15/1; $(P_H)_{Rup}$ = 4190 ksc.

FIGURE 12.—WARPED PLANE OF SHEARING, AT 16° TO 31° WITH THE AXIS OF A SOLID CYLINDER OF CAMBRIDGE SLATE
Spec. CS-12; P_H = 300 ksc; $(\sigma_D)_{Rup}$ = 5280 ksc.

FIGURE 13.—COPPER JACKETING DEPRESSED OVER "TRAP-DOOR" RUPTURE IN A HOLLOW CYLINDER OF SOAPSTONE
Spec. SP-1; α = 3.05/1; $(P_H)_{Rup}$ = 640 ksc.

FIGURE 14.—RUPTURE ALONG A TANGENTIAL-RADIAL SHEAR SURFACE IN A HOLLOW CYLINDER OF VERDE ANTIQUE ON THE SECOND TEST
In the first test there was a slight spalling for a hydrostatic pressure of 5620 ksc, which weakened the specimen. Spec. VA-22; α = 3.19/1; $(P_H)_{Rup}$ = 5000 ksc.

FIGURE 15.—SHEARING RUPTURE IN A HOLLOW CYLINDER OF CAMBRIDGE SLATE
Note tension cracks in the "hinge" at bottom. Spec. CS-8; α = 3.05/1; $(P_H)_{Rup}$ = 4670 ksc.

FIGURE 16.—SAW-TOOTH RIDGES ON THE TANGENTIAL-RADIAL SHEAR SURFACES OF A HOLLOW CYLINDER OF QUARTZ
Spec. Q-52; α = 3.19/1; $(P_H)_{Rup}$ = 8750 ksc.

required at 400° C to promote the inversion, and the pressure becomes higher with higher temperatures. (For recent experimental data on this system, *see* Jamieson, 1953.) Bridgman usage (Orowan, 1949, p. 186) as strength is usually applied only to ultimate resistance to rupture. As a geologic process, plastic flow is as important as fracturing in rocks.

TABLE 1.—PLASTIC DEFORMATION OF HOLLOW CYLINDERS OF SOLENHOFEN LIMESTONE AND YULE MARBLE UNDER HEAT AND PRESSURE

Specimen number	Ratio of radii	Hyd. press. (kg/cm²)	Temp. (°C)	Duration of experiment (hours)	Maximum decrease in O.D. (inches)	Normal rupture press. at 20°C* (kg/cm²)
S-10	2.50/1	2600	650°	3	.060	2400
S-24	2.55/1	2400	700°	2	.060	2450
S-34	2.40/1	1500	400°	20	<.001**	2350
		1700	400°	48	.002	....
S-25	2.35/1	1800	400°	50	.003	2300
S-42	2.40/1	2100	400°	56	.006**	2350
		3900 (Max.)	400°	1	Rupture	2500
S-43	2.40/1	1400	500°	20	<.001**	2350
		2000	500°	12	.016**	....
		5100 (Max.)	500°	7	.029	....
YM-15	2.38/1	1400	300°	2	Rupture	1350
YM-14	2.37/1	2100	400°	20	.097	1350
YM-16	2.40/1	600	400°	13	.001**	1400
		600	500°	12	.001**	....
		900	300°	12	.001**	....
		900	400°	12	.001**	....
		900	500°	12	.003**	....
		1100	400°	12	.002**	....
		900	400°	52	.002**	....
					(*Total* .013)	

* Normal hydrostatic pressure at rupture taken from Figure 7 and Yule marble curves.

** Measurement made on outside of copper jacket.

(1939) found a transition in calcite (Phase I–Phase II) at 15,000 ksc at room temperature, but this inversion also is too high to be important here. The vapor pressure of CO_2 from $CaCO_3$ is less than 20 mm Hg, for temperatures below 600° C, so dissociation effects are not important in the recrystallization and plasticity.

STRENGTH OF LIMESTONE

Definition of Strength

The initiation of plastic deformation at the elastic limit or the yield point is the subject of considerable research by metallurgists, and the word strength is often applied by them to the maximum stress difference at the elastic limit, although there are objections to this

The change in property at the elastic limit from elastic to plastic is here termed yield strength; rupture strength designates strength at rupturing. Yield and rupture failure describe loss of strength by yielding and by rupturing; yield failure may be a less acceptable usage, but beyond the elastic limit, there is a failure to continue elastic deformation.

Yield strength may be defined as that stress difference a body is able to withstand without yielding plastically, and may be arbitrarily designated as the maximum stress difference at the elastic limit or proportional limit for constant experimental conditions. Rupture strength may be defined as the maximum stress difference a body is able to withstand prior to loss of cohesion by fracturing for constant experimental conditions; fracturing is conceived as the breaking process leading to rupture. In

this study, nearly constant experimental conditions were maintained as follows: room temperature, unvarying composition, fresh, homogeneous specimens with no recent strain history, and moderate strain rate—about 0.02 per cent per minute. To conform with general usage (especially tests in air) stress difference is used as the measure of yield strength and rupture strength because either strength was found in this study to be more or less predictable for any rock by the magnitude of the maximum shear stress (half the maximum stress difference) at failure.

Goranson (1940, p. 1032) has proposed that strength (*i.e.*, yield strength) be measured by extrapolation of stress difference for finite rates of creep to zero creep rate. However, theoretically (Freudenthal, 1950, p. 138) at a temperature above zero absolute, for a finite stress difference, the rate of plastic strain should always be greater than zero, and careful long-period measurement does show extremely small inelastic strain in limestone at stresses well below the elastic limit. On the other hand, for most substances under usual experimental conditions, the strain rate does seem to approach zero for finite stress differences, as demonstrated forcefully by the confidence placed in structural steel, brick, and other building materials. Creep of Solenhofen limestone in air (Griggs, 1939, p. 234–236, Fig. 4) with 1400 ksc compressive load showed a shortening of 0.02 per cent in a year and a half, which was extrapolated to give 0.05 per cent in one million years. Since determination of the yield strength at zero creep rate involves considerable experimental uncertainty, the short term elastic limit may be taken as an approximate lower limit of unrecoverable strain to fit Goranson's definition.

Jeffreys (1924, p. 111) stated that the strength (*i.e.*, yield strength) of a material may be called "the critical stress difference, above which the rate of change of shape does not decrease when the time of application of the stress increases". Even at high temperatures and pressures, limestone would not be the viscous nor perfectly plastic material suggested as necessary in Jeffreys' definition, and so this measure of yield strength does not seem practical.

Griggs defined his term, fundamental strength (1936, p. 564, 557), as the maximum differential stress a body will withstand for infinite time without failing by rupture or deforming continuously. This definition does not differentiate between yield strength and rupture strength, whereas it does seem that a distinction between the two is necessary to treat the two types of strength in rocks.

Symbols

The following symbols are used:

General

- r radius
- σ stress normal to a surface
- τ shear stress
- P pressure
- ϵ strain normal to a surface
- U displacement
- E Young's modulus
- G modulus of rigidity
- μ Poisson's ratio
- K constant

Subscripts

- z axial
- t tangential or circumferential
- r radial
- i inside surface
- o outside surface
- p punch face
- e elastic deformation
- s plastic deformation
- B elastic-plastic boundary

Particular

- σ_1 maximum principal stress
- σ_2 intermediate principal stress
- σ_3 minimum principal stress
- P_H hydrostatic pressure
- P_p pressure on punch face
- σ_D stress difference
- σ_m mean stress
- τ_M maximum shear stress
- t thickness of disks
- l, r initial length or radius
- l', r' final length or radius
- α ratio of outside radius to any radius in a hollow cylinder, $\frac{r_0}{r}$

Stress Distribution in the Elastic Range

The idealized distribution of stress in a solid cylinder in compression is simple (Fig. 1a): on any particle in the cylinder there is a hydrostatic pressure plus an axial compression. The total axial pressure on the ends of the cylinder produces the axial stress σ_z, and is the maximum principal stress, σ_1. The stresses on a plane perpendicular to σ_z are the tangential and radial stresses, which are equal to the hydrostatic pressure.

$$\sigma_r = \sigma_t = P_H = \sigma_2 = \sigma_3$$

The axial stress can be considered equal to the sum of the hydrostatic pressure and the stress difference.

Eq. 1 $$\sigma_z = \sigma_1 = \sigma_D + P_H$$

The maximum shear stress is given by

Eq. 2 $$\tau_M = \tfrac{1}{2}(\sigma_1 - \sigma_3) = \tfrac{1}{2}(\sigma_z - P_H) = \tfrac{1}{2}\sigma_D$$

The mean stress or mean pressure is one-third the sum of the principal stresses for all stress systems.

Eq. 3 $$\sigma_m = \tfrac{1}{3}(\sigma_1 + \sigma_2 + \sigma_3) = \tfrac{1}{3}(\sigma_z + 2P_H)$$

The longitudinal strain in the solid cylinders was a shortening.

Eq. 4 $$\epsilon_z = \frac{l - l'}{l}$$

In the hollow cylinders, there was a hydrostatic pressure on the outside surfaces (Fig. 1b) and zero pressure on the inside surface, and the expressions for the stresses are as follows (*see* Love, 1944, p. 145–146):

Eq. 5 $$\sigma_t = \sigma_1 = P_H \cdot \frac{r_o^2}{r^2} \cdot \frac{r^2 + r_i^2}{r_o^2 - r_i^2} = P_H \frac{\alpha_o^2}{\alpha_o^2 - 1} \cdot \frac{\alpha^2 + 1}{\alpha^2}$$

Eq. 6 $$\sigma_r = \sigma_3 = P_H \frac{r_o^2}{r^2} \cdot \frac{r^2 - r_i^2}{r_o^2 - r_i^2} = P_H \frac{\alpha_o^2}{\alpha_o^2 - 1} \cdot \frac{\alpha^2 - 1}{\alpha^2}$$

Eq. 7 $$\sigma_z = \sigma_2 = P_H \cdot \frac{r_o^2}{r_o^2 - r_i^2} = P_H \frac{\alpha_o^2}{\alpha_o^2 - 1}$$

Each principal stress is a function of hydrostatic pressure and wall thickness. With r_i constant, wall thickness varies directly with ratio of radii.

$$\Delta r = r_o - r_i = r_i(\alpha - 1)$$

The shear stress in a hollow cylinder is maximum at the inside surface, where $r = r_i$, and $\alpha = \alpha_i = 1$

Eq. 8 $$\tau_M = \tfrac{1}{2}(\sigma_{ti} - \sigma_{ri}) = P_H \frac{\alpha_o^2}{\alpha_o^2 - 1}$$

The mean stress has the same value throughout the cylinder and also is equal to the maximum shear stress.

Eq. 9 $$\sigma_m = P_H \frac{\alpha_o^2}{\alpha_o^2 - 1}$$

In the disk tests (Fig. 1c), the deformation by shearing, and the average shear stress on a cylindrical surface within the disk under the edge of the punch is assumed to be the maximum shear stress.

Eq. 10 $$\tau_M = P_p \frac{r_p}{2t}$$

The critical principal stresses are developed under the edge of the punch also.

Eq. 11 $$\sigma_1 = \frac{P_p r_p}{2t} + P_H$$

Eq. 12 $$\sigma_2 = P_H$$

Eq. 13 $$\sigma_3 = -\frac{P_p r_p}{2t} + P_H$$

The mean stress in the disk is equal to the hydrostatic pressure.

Eq. 14 $$\sigma_m = P_H$$

Stress Distribution in the Plastic Range

The stresses in the plastic range of deformation are assumed to have the same orientation as the stresses in the elastic range for the solid cylinder and disk tests, even though the plastic strains are not simply related to the stresses.

In a hollow cylinder with closed ends, under hydrostatic pressure on the outside surfaces, the mechanism of plastic deformation probably

occurs about as follows. The first plastic flow is at the inside surface, and as the hydrostatic pressure is increased, a thicker portion of the inside wall flows inward; as the outside pressure

Eq. 19 $\sigma_{re} = \sigma_3 = \frac{\tau_M}{\alpha^2}(\alpha^2 \ln \alpha_B^2 - \alpha_B^2 + \alpha^2)$

Eq. 20 $\sigma_{ze} = \sigma_2 = 2\mu\tau_M(\ln \alpha_B^2 + 1)$

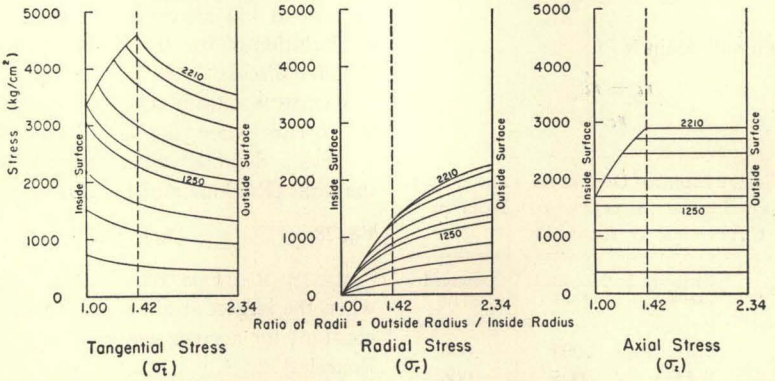

FIGURE 11.—THEORETICAL STRESS DISTRIBUTION IN THE WALL OF A HOLLOW CYLINDER UNDER EXTERNAL HYDROSTATIC PRESSURE

is further increased, the zone of plasticity widens into the wall of the cylinder. Outside this plastic zone, of course, the cylinder behaves elastically. In the actual tests, the widening of the plastic zone was interrupted by collapse in the thin- and medium-walled specimens and by spalling in the thick-walled specimens.

Beliaev and Sinitskii (1938) analyzed plastic flow in hollow cylinders; they assumed ideal plasticity, in which deformation is supposed to continue without increase of stress after reaching the yield point. They used Hencky's theory of plastic deformation in which the strain rate is not considered, and they assumed incompressibility in the plastic zone.

The stresses in the elastic and plastic zones in the wall of a closed hollow cylinder under external pressure is given by the following equations of Beliaev and Sinitskii. The maximum shearing stress is used to specify the condition for perfect plasticity.

Plastic zone:

Eq. 15 $\sigma_{ts} = \sigma_1 = 2\tau_M(\ln \alpha + 1)$

Eq. 16 $\sigma_{rs} = \sigma_3 = 2\tau_M \ln \alpha$

Eq. 17 $\sigma_{zs} = \sigma_2 = \tau_M(2 \ln \alpha + 1)$

Elastic zone:

Eq. 18 $\sigma_{te} = \sigma_1 = \frac{\tau_M}{\alpha^2}(\alpha^2 \ln \alpha_B^2 + \alpha_B^2 + \alpha^2)$

At plastic-elastic boundary.

Eq. 21 $\sigma_{tB} = \sigma_1 = 2\tau_M (\ln \alpha_B + 1)$

Eq. 22 $\sigma_{rB} = \sigma_3 = 2\tau_M \ln \alpha_B$

Eq. 23 $\sigma_{zB} = \sigma_2 = \tau_M(2 \ln \alpha_B + 1)$

In order to demonstrate the differences in the stress distributions between the elastic range and the plastic range, the curves in Figure 11 were drawn from the data on specimen S-115. In the three diagrams, the wall of the inside surface is on the left and the wall of the outside surface is on the right. The ratio of outside to inside radius for this specimen was 2.34/1, and intermediate ratios (for radii within the cylinder wall) are plotted along the abscissa. The ordinate axis shows the sizes of the tangential, radial, and axial stresses in ksc (kg/cm²). The two numbers, 1250 and 2210, on the curves are the external hydrostatic pressures observed at the elastic limit of the inside surface and at rupture. The curves below the 1250 curves show the stress distributions for wholly elastic deformation, and the curves above for elastic and plastic deformation. The elastic-plastic boundary at rupture was calculated to be at a radius ratio of 1.42/1.

The plastic strain at the inside surface, as observed in each manometer tube test and as computed from the theory, is given in Table 2 to show at least a rough correspondence between

experiment and theory for hollow cylinders. The theoretical tangential strain for the plastic range at the inside surface is

Eq. 24 $$\epsilon_{si} = \frac{U_{si}}{r_i} = \tau_M \frac{\alpha_B^2}{2G}$$

and the observed strain is

Eq. 25 $$\epsilon_{si} = \frac{r_i - r_i'}{r_i}$$

TABLE 2.—COMPUTED AND OBSERVED TANGENTIAL STRAINS AT INSIDE SURFACE OF HOLLOW CYLINDERS AT RUPTURE

Specimen no.	Ratio of radii	Computed strain	Observed strain
S-106	1.42/1	.005	.006
S-105	1.43/1	.005	.006
S-114	1.65/1	.005	.009
S-115	2.34/1	.008	.013
S-116	2.38/1	.007	.014
S-117	3.27/1	.009	.020
S-111	3.38/1	.009	.021
S-112	4.50/1	.011	.017
S-113	4.50/1	.011	.021

The maximum shear stress in the cylinder at rupture is at the plastic-elastic boundary (Eqs. 21 and 22, also Fig. 13).

$$\tau_M = \tfrac{1}{2}(\sigma_{tB} - \sigma_{BB})$$

Eq. 26 $$= \tfrac{1}{2}[2\tau_M (\ln \alpha_B + 1) - 2\tau_M \ln \alpha_B]$$

$$= \tau_M$$

The mean stress is greatest at the plastic-elastic boundary.

Eq. 27 $$\sigma_{m_B} = \tau_m(2 \ln \alpha_B + 1)$$

Criteria of Failure

A criterion of failure (either rupture failure or yield failure) for a given material may be defined as a quantitative statement which should be usable for all stress systems to predict either rupture or yielding, for given conditions of temperature, physical and chemical environment, and time. (A criterion should predict failure for *all* materials for the given conditions, but no such generality is possible at the present time.) The criterion may be based on the strain or the stress condition. Most of the criteria discussed here are phenomenological; the Griffith criterion is mechanistic in that failure at flaws in a substance is the basis of analysis. Neither type of criterion takes into account time effects, such as rate of loading, length of time under load, or in general the history of loading. A brief recapitulation of the criteria is given here (for a detailed discussion *see* Nadai, 1933).

MAXIMUM PRINCIPAL-STRESS CRITERION: Failure occurs when the largest principal stress reaches a definite value, constant for a given material (Rankine and Lamé).

Eq. 28 $$|\sigma_1| = K$$

MAXIMUM STRAIN CRITERION: Failure occurs when the largest strain reaches a critical value, constant for a given material (St. Venant and Poncelet).

Eq. 29 $$|\epsilon_1| = K$$

MAXIMUM SHEAR-STRESS CRITERION: A stressed solid commences to flow plastically or to rupture when the maximum shear stress exceeds a limiting value, characteristic of the solid (Coulomb and Tresca).

Eq. 30 $$\tau_M = \tfrac{1}{2}\sigma_D = \tfrac{1}{2}(\sigma_1 - \sigma_3) = K$$

INTERNAL-FRICTION CRITERION: Failure occurs when the shear stress plus the stress due to internal friction on a failure plane reaches a value which is constant for a given substance. This is an extension of the maximum shear-stress rule based on the assumption that the resistance of a specimen to fracture on the surface of slip was influenced by the normal pressure on that surface (Navier).

Eq. 31 $$\tau_n + F_1\sigma_n = K_1$$

which can be expressed also as

Eq. 31a $$\sigma_1 - F_2\sigma_3 = K_2$$

where F_1 and F_2 are functions of the "coefficient of friction", ϕ, on the slip plane, n,

$$F_1 = \phi \quad \text{and} \quad F_2 = \frac{\sqrt{\varphi^2 + 1} + 1}{\sqrt{\varphi^2 + 1} - \phi}$$

and ϕ is related to the plane of fracturing by

$$\phi = \cot 2\theta$$

where θ is the angle between the maximum principal stress and the fracture plane.

MOHR CRITERION: Failure occurs at a maximum shear stress on a failure plane determined by some function of the normal stress on that plane, which is a generalization including the maximum shear stress and internal friction criteria (Mohr).

Eq. 32 $$\tau_M = f(\sigma_n)$$

Mohr showed that the envelope to the circles of the Mohr diagram expresses geometrically the interdependence of the shear stress and of the normal stress on the failure plane, and he suggested that the envelope is a function of the angle between the fracture plane and the principal stresses. (*See* Nadai, 1950, p. 94–108.)

STRAIN-ENERGY CRITERION: Failure occurs by yielding or rupture when a constant amount of distortional strain energy is stored in an element of volume (Von Mises and Beltrami).

The failure condition is usually expressed in terms of the stresses rather than the strains,

Eq. 33 $$(\sigma_1 - \sigma_2)^2 + (\sigma_1 - \sigma_3)^2 + (\sigma_2 - \sigma_3)^2 = 2K^2$$

Alternatively, this criterion was given a geometrical representation by Nadai (1950, p. 209–211), from which he obtains the name, octahedral shear stress.

Eq. 33a $$\tau_{oct} = \tfrac{1}{3}[(\sigma_1 - \sigma_2)^2 + (\sigma_1 - \sigma_3)^2 + (\sigma_2 - \sigma_3)^2]^{\frac{1}{2}}$$

The distortional strain energy criterion has been found applicable to the yielding of ductile metals.

GRIFFITH CRITERION: Failure by fracturing is caused by stress concentrations at the tips of an elongated crack when the work done by the external forces exceeds the elastic plus surface energies stored at the crack (Griffith, 1925). With tensile stresses regarded as positive:

If $(3\sigma_1 + \sigma_3) > 0$ rupture occurs when

Eq. 34a $$\sigma_1 = K$$

If $(3\sigma_1 + \sigma_3) < 0$ rupture occurs when

Eq. 34b $$(\sigma_1 - \sigma_3)^2 + 8K(\sigma_1 + \sigma_3) = 0$$

where K is the same constant in both equations.

WEIBULL CRITERION: This criterion is based on an assumed normal frequency distribution for rupture strengths, determined statistically from many experiments of one type on similar specimens (Weibull, 1939; Frankel, 1948). Since the stress function of strength must be found empirically for each stress system, this criterion is not general, and it will not be discussed.

Yield Strength of Limestone

The criteria may be applied to predict the yielding of limestone in the various stress systems. In this investigation, the beginning of plastic flow has been assumed coincident with yielding at the elastic limit, and in turn the elastic limit has been chosen arbitrarily to coincide with the proportional limit, that is, at the point on a stress-strain curve at which linearity of strain with stress ceases; and yield strength has been defined in terms of the elastic limit.

The maximum principal-stress rule does not apply in the solid cylinder case because of the linear increase of the total axial pressure with increase of hydrostatic pressure (Fig. 3; Eq. 1). The maximum strains differ with the various stress systems (Figs. 3, 9, 10), and no mutual regularity was found. The Griffith factor, K, can be shown to vary inversely with hydrostatic pressure for constant stress difference in the solid cylinder tests (Fig. 3; Eqs. 1, 34b), so the Griffith criterion does not apply.

The internal friction and Mohr criteria coincide with the maximum shear-stress rule for yielding at the elastic limit. In Figure 12 are plotted points at the elastic limit taken from the stress-strain curves for Solenhofen limestone (Figs. 3, 9, 10) and recalculated to maximum shear stress (Eqs. 2, 8, 10) and mean stress (Eqs. 3, 9, 14). The standard deviation of the mean value of maximum shear stress is about 100 ksc. An extension of the maximum shear line to the right in 12 could be made for mean stresses of 19,000 ksc and 23,000 ksc from additional tests on two solid cylinders of Solenhofen limestone. The maximum shear stress from both tests was 1800 ksc, plus or minus 300 ksc. The accuracy of these values in the high-pressure tests is rather low because of the uncertain friction corrections in the apparatus used (not described here).

The maximum shear stress is constant for each of the very different stress systems, and therefore this criterion of yield strength is valid for Solenhofen limestone over a large range of mean stress. The validity of the criterion is

enhanced by the coincidence of the theoretical surface of maximum shear stress (Fig. 8b) and the actual surface of fracture in the hollow cylinders, assuming that the fracturing was propagated without distortion from the elastic zone through the plastic zone. The mechanical restraints on the solid cylinders and disks modified their modes of failure.

A plot of octahedral shear stress for the same data as in Figure 12 does not give any closer distribution of points around a critical value than that shown for maximum shear stress. Therefore, in view of the approximately constant relation between maximum shear stress and octahedral stress, only the maximum shear stress need be discussed; also, the accuracy of the experimental data does not warrant separate analysis.

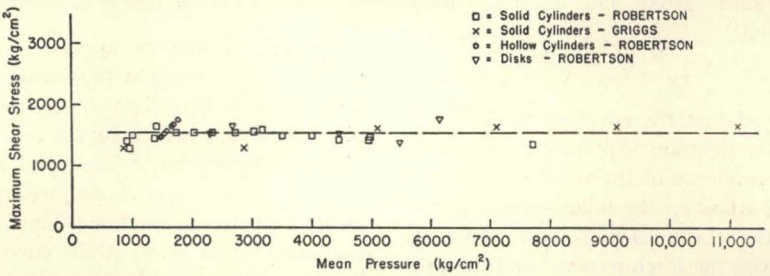

FIGURE 12.—MAXIMUM SHEAR STRESS VS. MEAN STRESS AT THE ELASTIC LIMIT, SOLENHOFEN LIMESTONE

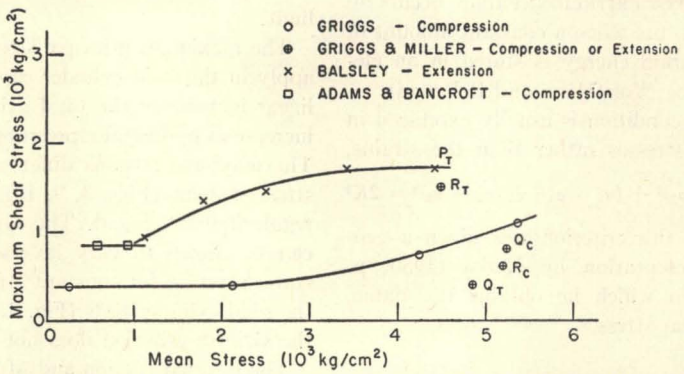

FIGURE 13.—MAXIMUM SHEAR STRESS VS. MEAN STRESS AT THE ELASTIC LIMIT, YULE MARBLE (GRIGGS AND MILLER, AND BALSLEY) AND CARRARA MARBLE (ADAMS AND BANCROFT)

The maximum shear-stress and the strain-energy criteria can be shown to be nearly equal in the numerical values of the yield condition. In the solid cylinder tests, the values of the principal stresses (Eq. 1) can be substituted in Equations 30 and 33a to give

$$\tau_{oct} = 0.94\,\tau_M$$

The same proportion between the values of the two criteria holds for any tension or compression tests and the punching tests on the disks for any hydrostatic pressure.

In the hollow cylinder tests (and for torsion tests), the values of the principal stresses (Eqs. 5, 6, 7) can be substituted in Equations 30 and 33a to give

$$\tau_{oct} = 0.82\,\tau_M$$

Although hydrostatic pressure has been used frequently for plotting of strength curves, mean stress is used here because it is a more general function.

Attempts to use the maximum shear-stress rule to evaluate all available reported tests on the strength of limestone or marble are given in Figures 13, 14, and 15; the points for the curves are computed from published and original data.

The circled-cross points in Figure 13 from Griggs and Miller (1951, Fig. 3) from tests on jacketed solid cylinders, bring out the anisotropy of strength caused by foliation. The lowest point, Q_T, represents an extension test in which

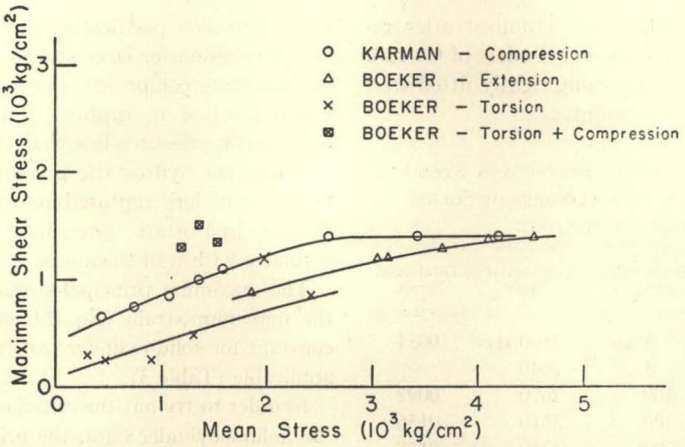

FIGURE 14.—MAXIMUM SHEAR STRESS VS. MEAN STRESS AT THE ELASTIC LIMIT, MARBLE (KARMAN AND BOEKER)

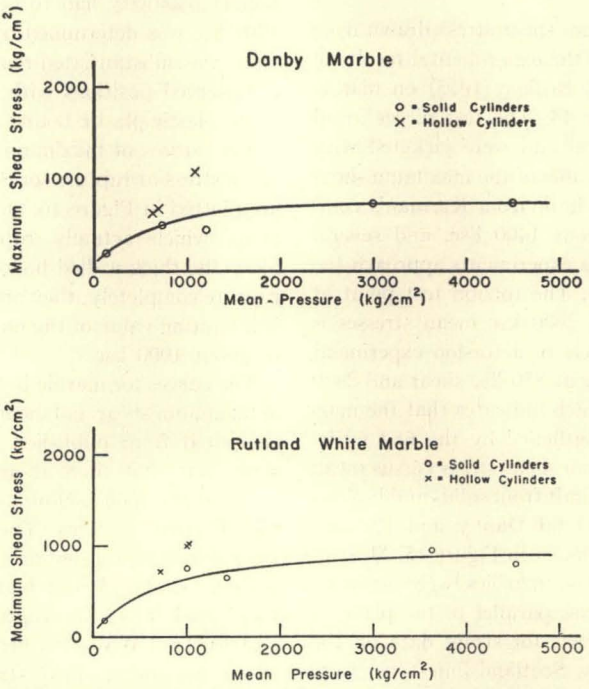

FIGURE 15.—MAXIMUM SHEAR STRESS VS. MEAN STRESS AT THE ELASTIC LIMIT, DANBY MARBLE AND RUTLAND WHITE MARBLE

the foliation of the specimen was perpendicular to a "tension" stress. The strongest orientation was that of P_T (Balsley, 1941, Fig. 6), perpendicular to R and to Q. Obviously, the yield strength of Yule marble depends on the orientation of the marble foliation and on the stress system used.

The curve in Figure 13 from Balsley's (1941, Fig. 4) experiments on jacketed, solid cylinders in extension approaches a limiting value of 1700 ksc which might be a limiting yield strength of the Yule marble for usual, room-temperature conditions. The curve from Griggs' (1936, Fig. 5) compression tests on an unknown marble may not be reliable because the solid cylinders were not jacketed. The two points from Adams

and Bancroft (1917) were obtained after recomputing their results on cylinders of Carrara marble in compression using tightly fitted steel jackets for lateral restraint.

TABLE 3.—TOTAL AXIAL STRESS AND STRAIN AT RUPTURE OF SOLID CYLINDERS OF SOLENHOFEN LIMESTONE

Specimen no.	Hydrostatic pressure	Total axial stress	Total axial strain
S-99	1 ksc	2800 ksc	.0034
S-55	1	2640	—
S-85	100	2670	.0092
S-83	300	3610	.0156
S-81	500	4240	.0168
S-82	700	4430	.0185

Curves of maximum shear stress drawn from curves and tables of the experimental results of Karman (1911) and Boeker (1915) on marble are shown in Figure 14. The test pieces in all cases were cylindrical and were jacketed with brass. The limiting value of the maximum shear stress at the elastic limit from Karman's compression tests is about 1400 ksc, and several points from Boeker's experiments approach the same limiting value. The torsion test point at 1200 ksc shear and 2000 ksc mean stresses is from the second cycle of a torsion experiment (the first cycle being at 850 ksc shear and 2420 ksc mean stress), which indicates that the marble was strain strengthened by the first cycle.

Curves of maximum shear stress versus mean stress at the elastic limit from solid- and hollow-cylinder experiments on Danby and Rutland White marbles are shown in Figure 15. Most of the cylinders of these marbles were oriented with the cylinder axes parallel to the plane of the foliation. The tests for strain data on the Becraft and the New Scotland limestones were too few to be conclusive.

Rupture Strength of Limestone

The quantitative analysis of the failure by rupture of a semiductile material like limestone is complicated by the plastic deformation that precedes the rupture.

Only the solid cylinders subjected to hydrostatic pressure less than 1000 ksc failed by rupture. Those tested at higher hydrostatic pressures deformed plastically with no important loss of cohesion for large strains and supported an increasing compressive load. The disk tests which resulted in rupture were those under hydrostatic pressures less than 3000 ksc; disks under higher hydrostatic pressures flowed. All hollow cylinders ruptured or spalled at well-defined hydrostatic pressures which varied regularly with wall thickness.

The maximum principal-stress (Eq. 28) and the maximum-strain (Eq. 29) criteria are not constant for solid-cylinder tests and so are not applicable (Table 3).

In order to try out the criteria of failure with the hollow-cylinder data, the principal stresses (Eqs. 15–23) had to be determined, and to do that a value of the shear-stress condition for perfect plasticity had to be found. A value of 1700 ksc was determined by curve-fitting; this value was substantiated roughly by comparison of observed positions with computed positions of the elastic-plastic boundary at rupture.

The curves of maximum shear stress versus mean stress at rupture for Solenhofen limestone are plotted in Figure 16. Only data from specimens which actually ruptured are plotted. Since the thick-walled hollow cylinders did not rupture completely, they are not plotted. There is a limiting value of the maximum shear stress of about 1900 ksc.

The curves for marble in Figure 17 are values of maximum shear and mean stresses at rupture computed from published results. It may be significant that there is an apparent limiting range (2000–3000 ksc) of maximum shear stress for all stress systems. The extension tests of Boeker and of Balsley are in close agreement, perhaps owing to the high hydrostatic pressures used. From the rupture data for Danby and Rutland White marbles and Becraft limestone, maximum shear stress at rupture approached but is less than that for Solenhofen limestone; New Scotland limestone was considerably stronger.

In order to test the Mohr (Eq. 32) and internal-friction (Eq. 31) criteria, a Mohr circle diagram from the experimental results of Karman and of Boeker (his extension tests only) is given in Figure 18; and Figure 19 is the diagram from my experiments on Solenhofen limestone. In both figures, only the data from speci-

mens which ruptured completely are plotted. If the Mohr criterion (or the internal-friction criterion) were valid, the envelope curves above the circles would be superimposed for all stress systems on a given material. Although unfortunately not plotted on Figure 18, it is evident from Figure 17 that a Mohr envelope of Boeker's torsion plus compression tests would lie much above the two envelopes shown. Boeker (1915) did his experiments to test the Mohr criterion, and he concluded that the Mohr criterion without correction did not satisfy both sets of data. Figure 19 suggests a similar conclusion.

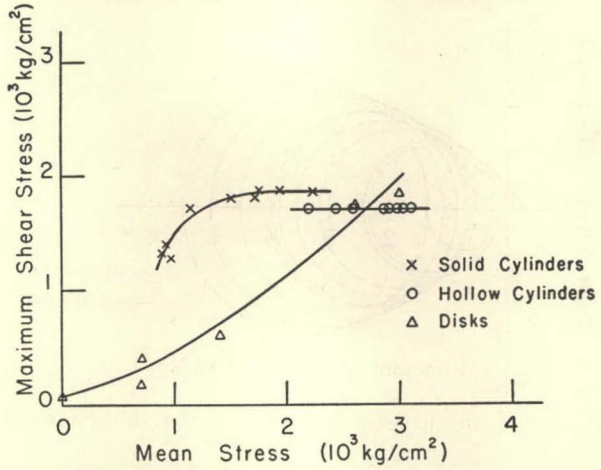

FIGURE 16.—MAXIMUM SHEAR STRESS VS. MEAN STRESS AT RUPTURE, SOLENHOFEN LIMESTONE

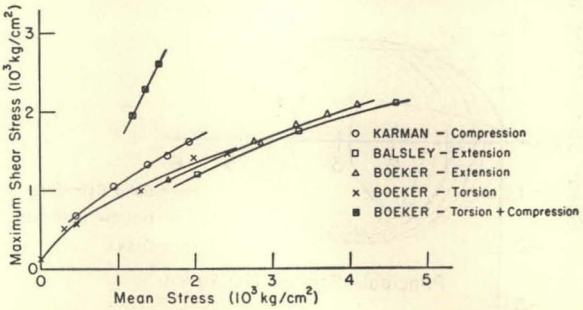

FIGURE 17.—MAXIMUM SHEAR STRESS VS. MEAN STRESS AT RUPTURE, MARBLE (KARMAN, BOEKER, AND BALSLEY)

Professor E. Orowan suggested that tension or bending tests on the limestone should be made as a check on the Griffith theory. (The check of the theory is in the comparison of the constant, K, found from a stress system in which Equation 34a applies with the K from a system in which Equation 34b applies.) Four rectangular bars of Solenhofen limestone were tested in an experimental set-up like that suggested diagrammatically in Figure 1d. The static load on a pan suspended from the middle of the bar was increased until the bar broke; there was no confining pressure.

A comparison of the rupture data from experiments on solid and hollow cylinders and on disks (using Eq. 34b) with the bending tests (using Eq. 34a) is made in Table 4. The values of the constant K, computed from the bending tests are listed with the values of K from the other tests. The values for K are scattered with some concentration between 300 and 400 ksc; there is a large variation of K with hydrostatic pressure in the disk tests. More experimental work is necessary to test this criterion thoroughly for rupture in Solenhofen limestone.

Conclusions on the Strength of Limestone

Limestone acts as a brittle material at low hydrostatic pressures and as a ductile material at high hydrostatic pressures. The boundary of hydrostatic pressure between the two types of behavior depends on the stress system involved: it is 1000 ksc for compression of solid cylinders, 3000 ksc for punching of disks, and about 6000 ksc for extension of solid cylinders.

The yield strength of Solenhofen limestone is nearly constant at 3200 ksc for mean pressures up to 23,000 ksc. The marble used by Karman and Boeker had an upper limit of the maximum shear stress at the elastic limit for their several stress systems of 1400 ksc. The upper limit of the maximum shear stress for Yule marble is about 1700 ksc. Generalizing, the yield strength of any fairly pure limestone or marble seems to have a consistent upper limit of about 3400 ksc for the nearly constant laboratory conditions, room temperature, slow strain rate, and constant chemical environment.

Rupture occurred in my experiments on Solenhofen limestone for limiting values of the maximum shear stress of 1700 to 1900 ksc. For marbles tested by Karman, Boeker, Balsley, and Griggs in compression, torsion, and extension, rupture occurred over a range of limiting maximum shear stress around 2000 ksc. In terms of stress difference, the limiting rupture strength of limestone and marble is about 4000 ksc for the nearly constant laboratory conditions.

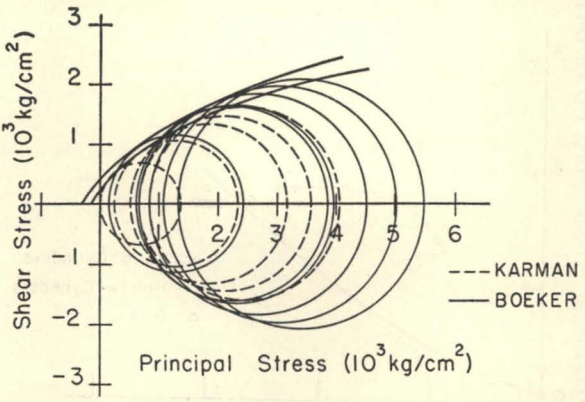

FIGURE 18.—MOHR DIAGRAM OF THE RESULTS BY KARMAN AND BY BOEKER ON RUPTURE OF MARBLE

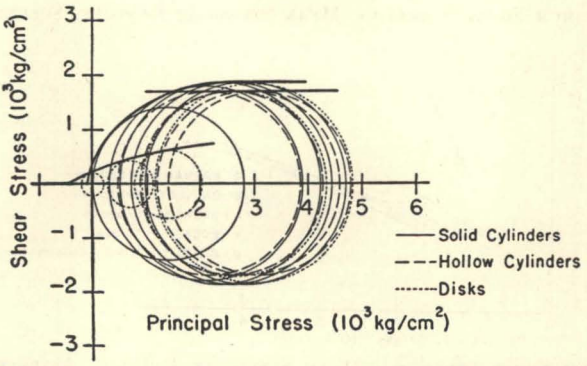

FIGURE 19.—MOHR DIAGRAM OF THE RESULTS ON RUPTURE OF SOLENHOFEN LIMESTONE

The observed and theoretical rupture strengths of ionic crystals differ markedly. Polanyi (1921) and Zwicky (1923) determined for sodium chloride a theoretical tensile strength by rupture of about 10,000 ksc; the measured strength is about 50 ksc. Frankel's approximation (Orowan, 1940, p. 12) for shear strength

of ionic crystals is:

Eq. 35 $$\tau_N = \frac{G}{2\pi}$$

For limestone this expression gives a theoretical maximum shear stress of about 40,000 ksc, which is 20 times the limiting stress I observed. Bridgman's shearing test on Solenhofen limestone (Birch *et al.*, 1942, p. 127) shows that the shearing stress at the knee of his curve is about 7000 ksc for a hydrostatic pressure of about 30,000 ksc. It is possible that Bridgman was testing at least approximately the atomic forces holding welded calcium carbonate grains together.

TABLE 4.—STRENGTH CONSTANT OF GRIFFITH CRITERION OF FAILURE FROM EXPERIMENTS ON SOLENHOFEN LIMESTONE

Specimen type	Specimen no.	Hydrostatic pressure (ksc)	K (ksc)
Bar (Bending)	S-95	1	380
	S-96	1	400
	S-97	1	420
Solid cylinder (Compression)	S-99	1	350
	S-85	100	230
	S-83	300	390
	S-81	500	370
	S-82	700	340
	S-86	1000	300
Hollow cylinder (Compression)	All	—	400
Disk (Punching)	S-100	1	0
	S-101	700	60
	S-118	1400	70
	S-92	2600	290
	S-91	3000	280

EXPERIMENTAL RESULTS FOR SILICATE ROCKS AND MINERALS

Introduction

An attempt was made to determine some regularity in the strengths of silicate rocks and minerals. The same experimental techniques used in testing solid cylinders and hollow cylinders of limestone (Figs. 1a, 1b) were employed on twelve igneous, sedimentary, and metamorphic rocks, and on four minerals. The problems engendered by such physical characteristics as foliation, grain size, mineralogic and chemical composition, porosity, and moisture content were not evaluated.

Results from Solid-Cylinder Compression Tests

The stress-strain curves from experiments on igneous rocks are uniform in being elastic almost to the point of rupture. Furthermore, the effect of hydrostatic pressure seems to be the same for each rock: a marked increase in strength occurs with increasing hydrostatic pressure. The sedimentary and metamorphic rocks and the minerals tested all behaved in much the same way. Since these rocks are all brittle under the nearly constant laboratory conditions used, only their rupture strengths could be investigated.

Stress-strain curves from tests on solid cylinders of Barre granite, Cambridge slate, and pyrite are shown in Figure 20. (*See* Appendix 1 for rock descriptions and symbols.) The increase in the rupture strength with increasing hydrostatic pressure is obvious. Planar shear surfaces at angles less than 45° to the cylinder axis seem common to all specimens, with wedging failure in some specimens (Pl. 4, figs. 1, 2, 9, 12).

In view of the plasticity of limestone and marble, a series of experiments on solid cylinders of dolomite was performed for a large range of hydrostatic pressure (Fig. 21). Unlike limestone, the Blair dolomite is brittle, although for very high hydrostatic pressure evidence of plastic flow was observed; the permanent set in BD—6 was 0.8 percent. The rupture of the other specimens was typically brittle, a wedging and planar shearing failure.

Results from Hollow-Cylinder Tests

Owing to limitations in the strength of the apparatus, it was not possible to break solid cylinders of silicate rocks at hydrostatic pressures higher than about 1000 ksc (kg/cm^2). Decreasing the size of the specimen to cause rupture would introduce inhomogeneities from the individual mineral grains. To obviate this problem, most of the tests were run on hollow cylinders, since higher stress differences could be attained. One test was made on each rock using the manometer tube to measure the strain at the inside surface. The mode of failure of the medium-walled hollow cylinders (Pl. 4), as in the limestones and marbles, was along the theoretical tangential-radial shear surface (Fig. 8b); the thin-walled cylinders disintegrated upon collapse.

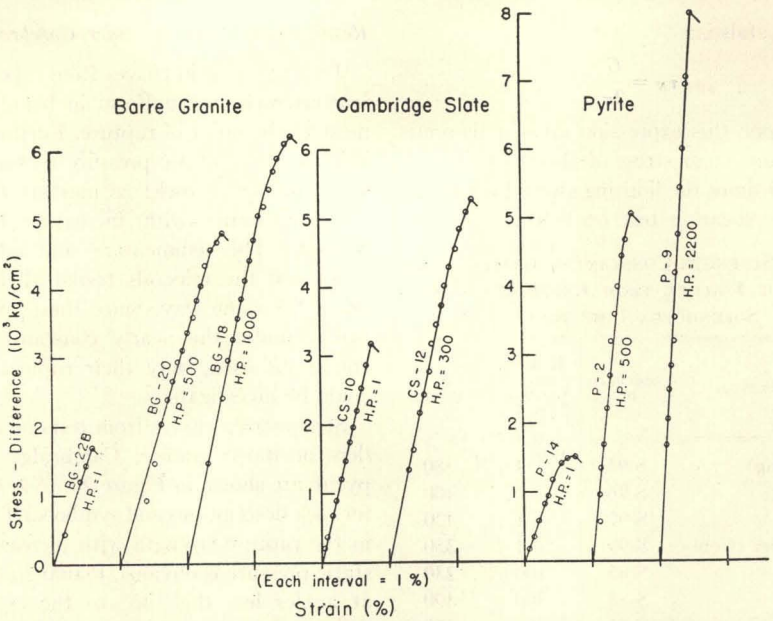

FIGURE 20.—STRESS-STRAIN CURVES FROM AXIAL-COMPRESSION EXPERIMENTS ON SOLID CYLINDERS OF GRANITE, SLATE, AND PYRITE

Each curve starts at zero strain; H.P. = hydrostatic pressure in kg/cm².

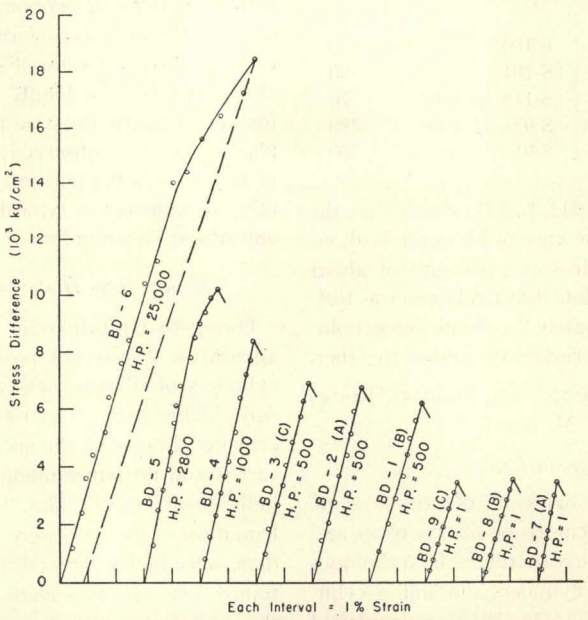

FIGURE 21.—STRESS-STRAIN CURVES FROM AXIAL-COMPRESSION EXPERIMENTS ON SOLID CYLINDERS OF BLAIR DOLOMITE

Letters A, B, and C refer to three mutually perpendicular axes.

The hollow cylinders of the sedimentary and metamorphic rocks and of the minerals ruptured like the igneous-rock cylinders, and in fact all these geologic materials had about the same rupture strength (Fig. 22), although sandstone (GS and RS), soapstone (SP), and quartz (Q) are important exceptions.

Strain data from the manometer tests on the

hollow cylinders showed good agreement with the theoretical strains for all rocks except microcline and red sandstone, which may be explained by erratic errors in the apparatus.

cylinder tests, and so the Griffith criterion is not applicable to silicate rocks. Bridgman (1947a, p. 257–258) pointed out that Griffith's concept of microscopic failure by intensified

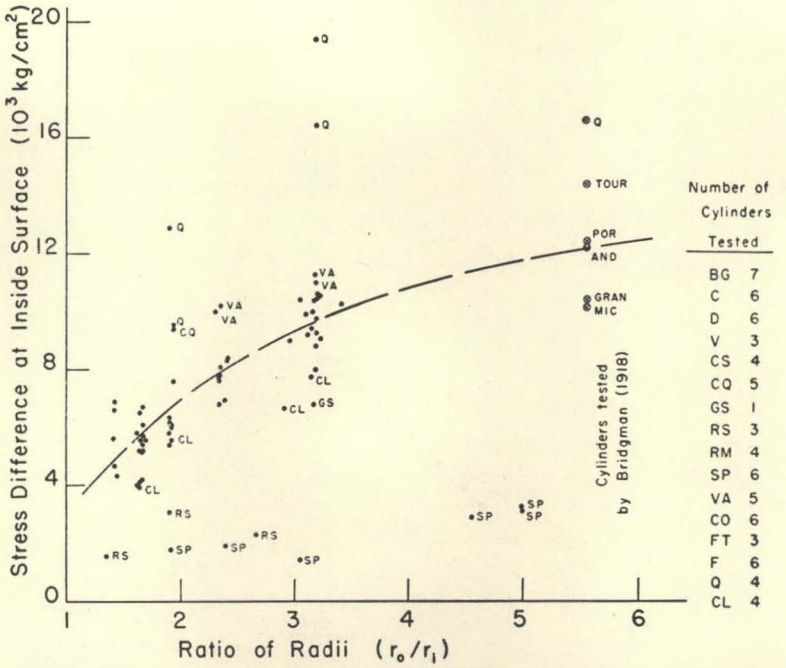

FIGURE 22.—SCATTER DIAGRAM OF RUPTURE STRENGTH VS. RATIO OF RADII FOR CRUSHING TESTS OF HOLLOW CYLINDERS OF SILICATE ROCKS AND MINERALS

Application of Criteria of Failure to Silicate Rocks

The most significant difference in behavior between the limestone and the silicate rock specimens is the complete lack of any important plastic flow phenomena in the silicate rocks. This thoroughly brittle behavior at room temperature of the silicate rocks and minerals is a marked feature of these materials for moderate hydrostatic pressures.

The usefulness of the criteria of failure can be tested for prediction of rupture of silicate rocks. The maximum principal-stress (Eq. 28) and maximum principal-strain (Eq. 29) criteria do not apply to rupture of silicate rocks, because these quantities increase with increasing hydrostatic pressure (Fig. 20). As for the Griffith criterion, values of K from the solid-cylinder and hollow-cylinder experiments on Barre granite are listed in Table 5; the value of K for granite in tension is 50 ksc. With increasing hydrostatic pressure, K increases linearly in the hollow-

TABLE 5.—STRENGTH CONSTANT FROM GRIFFITH CRITERION OF FAILURE FROM EXPERIMENTS ON BARRE GRANITE

Specimen no.	Max. prin. stress (ksc)	Min. prin. stress (ksc)	K (ksc)
Solid cylinders			
BG-22B	1700	0	210
BG-17B	4500	500	400
BG-20	5150	550	470
BG-18	6100	1000	460
Hollow cylinders			
BG-3	3800	0	480
BG-4	3600	0	460
BG-1	4400	0	540
BG-9	5200	0	640
BG-10	5000	0	620
BG-6	7000	0	880
BG-5	7600	0	960

stresses in cracks is oversimplified for the macroscopic, average nature of stress and strain.

The Mohr, internal-friction, and maximum shear-stress rules for failure (Eqs. 30, 31, 32) do not apply to these silicate rocks as found from Mohr circle plots of the rupture data. The Mohr circles for stresses at rupture for hollow cylinders are mutually tangent at the origin, although of increasing diameter (an increasing function of wall thickness), and no common envelope can be drawn between circles from hollow-cylinder and solid-cylinder data.

An effort was made to find a functional relationship between the maximum stress difference (rupture strength) and any other parameter in order to predict the rupture strength of the silicate rocks. A fairly satisfactory relation was found, which affords a rough approximation and which is given by a direct proportionality between maximum shear stress (half the maximum stress difference) and mean stress.

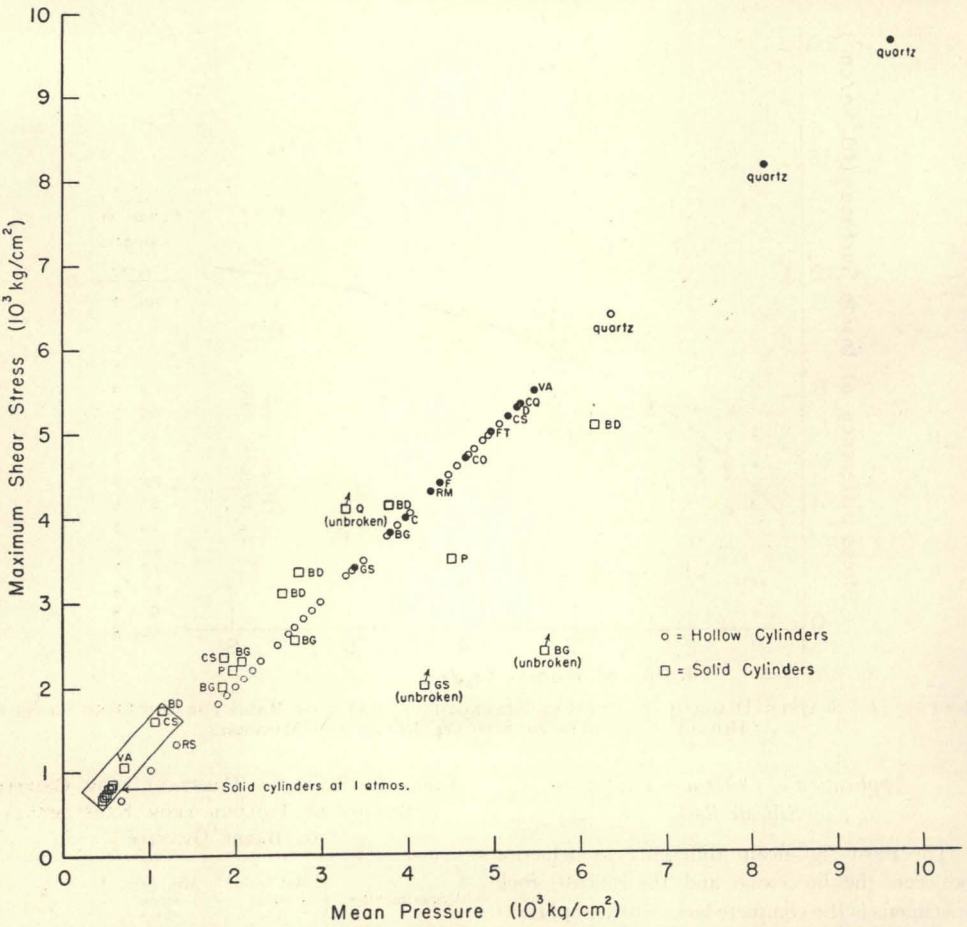

FIGURE 23.—MAXIMUM SHEAR STRESS VS. MEAN STRESS AT RUPTURE, VARIOUS ROCKS AND MINERALS

Eq. 36 $$\tau_M \cong \sigma_M$$

Certain mathematical errors are inherent in this approximation for certain stress systems. In Bridgman's "pinching-off" tests, in which the radial and tangential pressures on a solid cylinder are equal and the axial stress is zero, the approximation reduces to an identity in which the ratio τ_M/σ_m becomes 0.75 instead of 1.00. In axial tension or compression tests *in air*, the approximation reduces to another iden-

tity in which τ_M/σ_m becomes 1.50 instead of 1.00; however, for lateral pressures greater than zero, the identity need not hold.

Figures 22 and 23 strongly suggest that for the well-indurated rocks and for certain minerals the rupture strength of each is a function

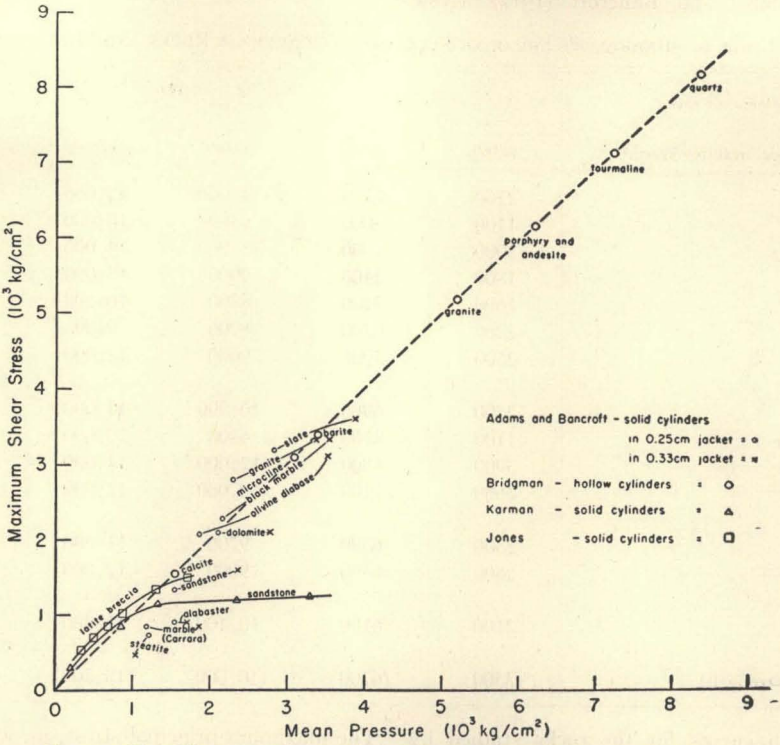

FIGURE 24.—MAXIMUM SHEAR STRESS VS. MEAN STRESS AT RUPTURE

From Experiments by Adams and Bancroft, Karman, Bridgman, and Jones on various rocks and minerals.

Rupture Strength of Silicate Rocks

A composite plot of data from all rocks and minerals I tested is given in Figure 23, which shows the apparent relation at rupture between the two parameters, τ_M and σ_m (Eq. 36). This equality is overemphasized for hollow cylinders in the straight line of Figure 23 because they are equal only according to first-order elasticity theory (Eqs. 8, 9); and the analysis used for the hollow-cylinder case cannot be applied too closely to rocks, because the elasticity of rocks is inexact compared to the mathematical model. (Circles for a radius ratio of about 3.2/1 are blackened in Figure 23.)

For all the variety of geologic materials in Figure 23 none of the rocks and minerals exhibits the limiting rupture strength preceding plasticity found in the experiments on limestone.

of the magnitudes of the stresses but not of the stress system nor of the composition of the rock. This is only tentative, in view of the scatter of the points in Figures 22 and 23, and should be used only as a first, rough outline of the behavior of these rocks.

Quartz is extraordinarily strong. The experiment represented in Figure 23 by the solid-cylinder point at shear stress 4100 ksc and mean stress 3300 ksc was run at a hydrostatic pressure of 600 ksc, and a maximum stress difference of 8200 ksc was reached without breaking the cylinder. In Bridgman's (1941, p. 468–469) last-reported compression test on a solid cylinder of quartz, the sample ruptured at a maximum shear stress of 20,000 ksc and mean stress of 37,000 ksc, which is a point well below the 45° line.

The results of tests on various rocks and min-

erals taken from the literature are shown in Figure 24, including the work of Karman (1911), of Bridgman (1918), of Jones (1945), and of Adams and Bancroft (1917). (New

Substituting in Equation 36,

Eq. 36a $$\tau_M \cong \tfrac{1}{3}(\sigma_1 + \sigma_2 - \sigma_2) \cong \tfrac{1}{3}\sigma_1$$

TABLE 6.—BRIDGMAN'S SHEARING STRENGTHS FOR SEVERAL ROCKS AND MINERALS

Mineral or rock	Shearing strengths (kg/cm²)				
(confining pressure—kg/cm²)	10,000	20,000	30,000	40,000	50,000
Anorthite	2200	7700	11,000	14,000	14,000
Augite	1100	3000	6300	10,000	13,000
Basalt glass	3000	7600	13,000	14,000	17,000
Bronzite	1800	3400	9000	13,000	16,000
Cassiterite	1600	5100	8300	10,500	12,500
Cuprite	2200	6200	8200	9400	10,300
Diopside	2500	5900	9000	12,000	14,000
Garnet	....	....	....	....	15–19,000
Hematite	2300	6900	10,900	14,000	16,700
Hornblende	1100	3100	6400	10,000	13,000
Obsidian	3900	8000	12,000	14,000	15,000
Opal	3600	7100	10,000	12,000	18,000
Quartz	....	....	....	....	14,500
Pyrite	2300	6300	9700	11,500	12,500
Pyroxenite	2800	6400	9000	12,000	14,000
Sericite	....	....	....	....	13,000
Sillimanite	2100	6100	10,100	11,200	11,800
(Predicted strength)	(3300)	(6700)	(10,000)	(13,300)	(16,700)

stress-strain curves for the rocks studied by Adams and Bancroft were plotted after recomputing the numerical data given. The pronounced yielding at the elastic limit was assumed to occur at the beginning of rupture of the sample which was much below the elastic limit for the steel jacket. The accuracy of the value of the lateral pressure of the jacket is difficult to appraise but it may be as good as plus or minus 100 ksc.)

The curve of points for tests on volcanic breccia by Jones (1945) shows a falling off like the sandstone of Karman, and like the Blair dolomite in Figure 23. The decrease in rupture strength as the mean stress is increased may mean that these materials will deform plastically at room temperature if the hydrostatic pressure is high enough.

Bridgman (1935; 1936; 1937) measured the shearing stress directly in his shearing experiments; and the principal stresses for his stress system are related as follows.

$$\sigma_1 > \sigma_2 = -\sigma_3$$

The maximum principal stress, σ_1, was that of the pressure across the disk of the specimen. The relationship expressed by Eq. 36a holds fairly well for Bridgman's shearing data as listed in Table 6, (taken from Table 9-7 Birch *et al.*, 1942, p. 126–128) especially at the higher confining pressures. Bridgman's data fit the empirical relation (Eq. 36) surprisingly well for such very high pressures. Evidently the powders (used to make up Bridgman's disks for shearing) of these rocks and minerals act like solid specimens with regard to strength at these high confining pressures.

Equation 36 may also be restated in terms of a hydrostatic pressure and the maximum shear stress in systems where two of the principal stresses are equal and less than the third (as in the solid cylinder compression tests).

$$\sigma_1 > \sigma_2 = \sigma_3 = P_H$$

then

$$\tau_M \cong \tfrac{1}{3}[(\sigma_1 - \sigma_3) + \sigma_2 + 2\sigma_3]$$

Eq. 36 b $$\tau_M \cong 3\,P_H$$

or

$$\sigma_D \cong 6\, P_H$$

The fit of the data from solid cylinder tests to Equations 36 and 36b can be seen in Figures 23 and 24.

For the extension-stress system, in which two principal stresses are equal and greater than the third:

$$\sigma_1 = \sigma_2 = P_H > \sigma_3$$

Substituting in Equation 36,

$$\tau_M = \tfrac{1}{3}[-(\sigma_1 - \sigma_3) + \sigma_2 + 2\sigma_1]$$

Eq. 36 c $$\tau_M \cong \tfrac{3}{5} P_H$$

or

$$\sigma_D \cong \tfrac{6}{5}\, P_H$$

The stress situation at rupture given by Equation 36c would be realized when the "tensile" stress difference was about equal to the hydrostatic pressure. Very few extension tests on brittle rocks have been made. However, there are a few tests on silicate materials which may be inspected. Bridgman (1947a, p. 250) found the rupture of Pyrex glass under a hydrostatic pressure of 27,000 ksc to occur at a "tensile" stress difference of 24,500 ksc, which agrees roughly with the prediction of Equation 36c. However, for synthetic sapphire, the stress difference at rupture was about one-fifth the hydrostatic pressure of 27,400 ksc; and for pipestone and for sodium chloride, the stress difference at rupture was about one-sixtieth of the hydrostatic pressure of 27,400 ksc. Boeker's and Balsley's extension tests on marble showed the stress difference at rupture to be about half the hydrostatic pressure.

The results of the "pinching-off" tests may be tried as an extension stress system by assuming Equation 36c to apply for small σ_3 greater than zero. Rupture of Pyrex glass rods by "pinching-off" occurs at a hydrostatic pressure of about 1600 ksc (P. W. Bridgman, personal communication), which is about equal to its maximum observed tensile strength in air; however, the strength of glass in both types of tests is notoriously variable. Richart, Brandtzaeg, and Brown (1928) found that concrete cylinders "pinched-off" at a hydrostatic pressure about equal to the compressive strength of the concrete in air, which might be taken as the maximum possible tensile strength of concrete, although extremely difficult to attain with the usual tension techniques.

Although there seems to be some experimental support for Equation 36 and its derivations, it is evident that this criterion of failure by rupture is empirical and only approximate. It does bring out an apparent dependence of strength on the sum of the stresses for silicate rocks.

Generalizations on Rock Strength

Strength (both yield and rupture) is an average, macroscopic property of materials, and for this reason only reasonably homogeneous materials tested in the same manner give reproducible strengths. Solenhofen limestone is remarkably uniform and isotropic for a rock and does give consistent yield and rupture strength results, but a moderate change in the testing conditions was found to change both strengths considerably. The yield and rupture strengths of a substance are affected by several factors: stress conditions, temperature, composition, chemical environment, physical character, deformation history, and strain rate.

Both yield and rupture strengths of rocks are defined and can be predicted in terms of stress differences but the sum of the stresses seems to be an independent factor in affecting strength. Hydrostatic pressure causes brittle limestone to become ductile, and it raises the rupture strength of silicate rocks markedly. Mean stress is a more general stress function and may be more significant than hydrostatic pressure for geologic processes near the surface of the earth.

Although the yield strength of limestone is constant for the standard conditions of this study, it is lowered by heating. The yield strength of Yule marble was found by Griggs *et al.* (1951, Fig. 1; 1953, Fig. 1) to be about 2500 ksc at 20° C and about 1000 ksc at 150° C and at 300° C. The values are for marble specimens in one orientation under hydrostatic pressure of 10,000 ksc.

Rupture in limestone on the other hand, seems to be deferred by heating in that there is a promotion of ductility in the limestone (Table 1). By analogy it may be postulated that heating will promote plasticity in silicate rocks, and Griggs (1954) has reported it in preliminary results for several silicate rocks.

A comparison of stress-strain curves of hollow cylinders of carbonate and silicate rocks and minerals is given in Figure 25, showing either yield strengths or rupture strengths. The

Yield and rupture strengths are sensitive to perfection and type of crystal structure, and to the state of aggregation of the mineral grains in a rock. All inhomogeneities in a rock grading

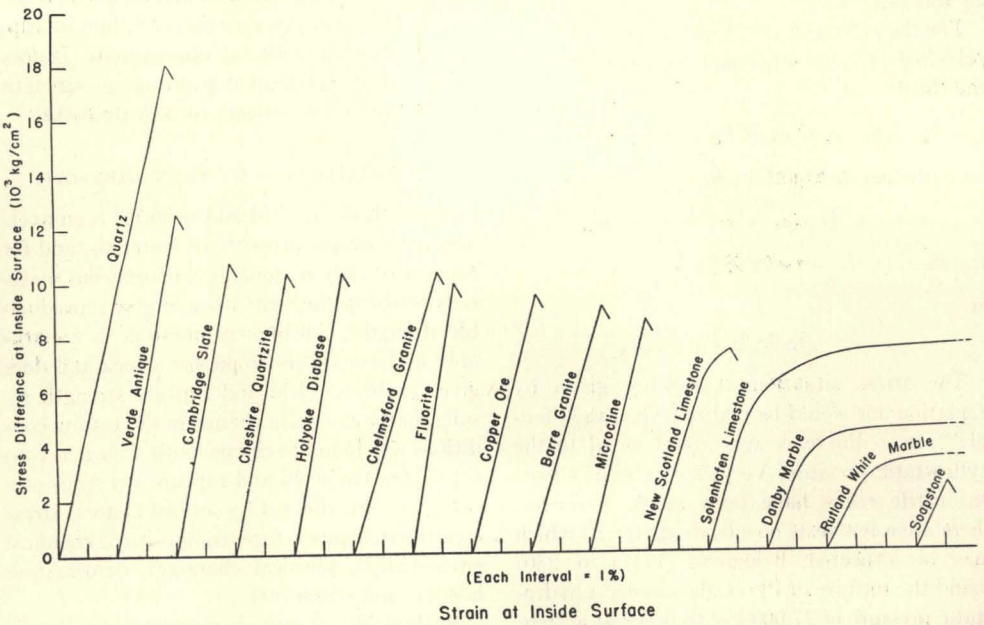

FIGURE 25.—COMPARISON OF RUPTURE STRENGTHS AND OF YIELD STRENGTHS FOR CRUSHING OF HOLLOW CYLINDERS OF THE SAME RATIO OF RADII

Curves were estimated from results on cylinders of nearest sizes.

contrast in behavior of the limestones and marbles with the silicate rocks and minerals is obvious, and the uniformity of rupture strengths of the silicate rocks is indicated (also Fig. 22).

The chemical environment is important, as shown by the experiments of Griggs (1940) on the deformation of gypsum under dry and under wet conditions, and the experiments of Joffe (1928) on salt under dry and wet conditions. Their results show that the effects of water on rupture strength may be due to chemical causes (e.g., recrystallization) or to physical causes (e.g., mechanical weakening) or both. The presence of water seems to strengthen salt by recrystallization, but it weakens gypsum mechanically. Mechanical weakening was shown in the variation of Young's modulus with moisture content by Delaney (1940); the modulus was halved by soaking a slab of soapstone in water, and the modulus came back as the slab dried out.

from imperfections inside mineral grains to inter-granular pores, and to foliations and joints, determine the effects of physical character on strength, and in general each imperfection weakens the rock. There is no reliable means at the present time of measuring the state of imperfection of a rock, so this is empirical and *a priori* reasoning.

The history of deformation (indicated by folding, jointing, and faulting) obviously affects the present rupture strength of a large mass of rock. Strain-strengthening effects from a history of cyclic deformation seem to be important in determining the yield strength of limestone but have not been studied adequately for limestone nor at all for silicate rocks.

A fast rate of loading causes the yield strength of limestone to be raised considerably, although it relaxes quickly.

An exponentially diminishing strain rate occurs in laboratory creep tests of limestone

(Griggs, 1939) for a static stress difference below the yield strength. However, creep of carbonate or silicate rock in the earth under a stress difference less than the yield or rupture strength cannot be evaluated very well in the laboratory, since the experiments are concerned with such minute time periods compared to geologic time. Bridgman (1936, p. 666) commented on this dilemma and on time effects in general, saying:

". . . I think we should not be frightened by the bogy of even geological time, but in our speculations freely use such concepts as shearing strength, admitting that the apparent strength in 10 million years may be a little lower than for laboratory experiments, or the strength for 100 million years a little lower than for 10 million, and also recognizing that the difference between geological and laboratory behavior may be a strong function of the material."

Appendix 1: Descriptions of Rocks and Minerals

Carbonate Rocks

(L) *Becraft limestone.*—The blocks of the Becraft limestone were obtained from a quarry at Alsen, New York. The rock is highly fossiliferous, the fossils in white calcite being clearly outlined in the reddish matrix, but thoroughly cemented into the matrix. It is a fairly pure limestone of early Devonian age. All test cylinders were cut with axes noraml to the bedding of the limestone.

(BD) *Blair dolomite.*—"Blair" is the local name for a dolomite from the Millville quarry at Martinsburg, West Virginia. The rock is a fine-grained, pure calcium-magnesium carbonate. Cylinder axes were cut in three perpendicular directions, (A, B, and C in Fig. 21).

(DB) *Danby marble.*—"Danby" is the trade name of the marble quarried at Danby, Vermont. The marble is a medium-grained (0.1 mm) white calcite marble, and is quite pure calcium carbonate; the impurities are 0.1 per cent Al_2O_3 plus Fe_2O_3, and 0.4 per cent MgO. The Danby marble is quarried from the Beldens formation of middle Ordovician age (Chazy). All test cylinders were cut with axes subparallel to the foliation.

(CL) *New Scotland limestone.*—The New Scotland limestone blocks were also obtained from the quarry at Alsen, New York. The fine-grained dark-gray New Scotland limestone is shaly. The argillaceous content is of the special mixture which makes the limestone a natural cement rock, and which accounts for the quarrying activity. An approximate chemical analysis of this early Devonian rock is 20 per cent SiO_2, 2 per cent Al_2O_3, 1 per cent MgO, 5 per cent FeO, and 72 per cent $CaCO_3$. The cylinders for test specimens were cut with axes normal to the bedding of the limestone.

(WM) *Rutland White marble.*—The name, "Rutland White", is the trade name of the Vermont Marble Co. for a high-grade statuary marble, quarried at West Rutland, Vermont. The impurities in the medium-grained marble are 0.1 per cent Al_2O_3 plus Fe_2O_3, and 0.3 per cent MgO. The Rutland marble is also taken from the Beldens formation. Axes of cylinders for testing were drilled in three directions.

(S) *Solenhofen limestone.*—The Solenhofen limestone has been considered one of the finest lithographic stones available. The original source of the limestone was Solenhofen, Bavaria. It is a buff-colored, extremely fine-grained (0.005 mm) limestone of fairly high purity. In addition to $CaCO_3$, the limestone contains 0.2 per cent Al_2O_3, 0.3 per cent FeO, 0.6 per cent MgO, 0.1 per cent K_2O and Na_2O, and 0.2 per cent H_2O at 100° C and 0.7 per cent H_2O at more than 100° C. The age is Jurassic. The test cylinders were cut in three orthogonal directions, but the orientation with respect to the original bedding is unknown.

(WHB) *William Henry Bay marble.*—The Wm. Henry Bay marble specimen was obtained from an outcrop in a small inlet of the same name, off the Lynn Canal and about 20 miles south of Haines, Alaska. The marble is a white, medium-grained (0.5–1.5 mm) rock. Chemical analyses of a marble which is presumed to be the same formation indicated that the Wm. Henry Bay marble is quite pure calcium carbonate. The age can only be tentatively set as early Paleozoic. The attitude of any foliation is not known.

(YM) *Yule marble.*—The Yule marble used was obtained from a quarry in Gunnison County, Colorado. The rock is a medium-grained, white marble of nearly pure calcium carbonate. The clear ellipsoidal grains form a granoblastic fabric. The age is Mississippian. Test cylinder axes were shaped in three perpendicular directions at odd angles with the foliation.

Igneous Rocks

(BG) *Barre granite.*—The Barre granite was obtained from the Rock of Ages quarry near Barre, in north central Vermont. The rock is medium- to coarse-grained (feldspar phenocrysts up to 5 mm in diameter) and medium gray in color. It contains orthoclase and microcline (about 45 per cent), light smoky quartz (about 25 per cent), oligoclase, plagioclase (about 20 per cent), biotite and some

muscovite (about 10%.) with small amounts of pyrite, magnetite, sphene, epidote, zircon, and rutile. The chemical composition is about 70 per cent SiO_2, 15 per cent Al_2O_3, 2.5 per cent FeO and Fe_2O_3, 1 per cent MgO, 2 per cent CaO, 5 per cent Na_2O, and 4 per cent K_2O. Test cylinders were cut with axes normal to the foliation of the granite.

(C) *Chelmsford granite.*—The blocks of Chelmsford granite were obtained from the quarry at West Chelmsford, Massachusetts. The rock is fine- to medium-grained and light gray. It is composed of microcline, quartz, and oligoclase, plagioclase, minor muscovite, and a little biotite, with accessories of magnetite, apatite, zircon, fluorite, and calcite. Test cylinders were shaped with axes normal to the foliation of the granite.

(D) *Holyoke diabase.*—The Holyoke diabase blocks were obtained from a quarry near Westfield, Massachusetts. The diabase is a dark-gray, very dense, fine-grained rock with broad conchoidal fracture; it is composed essentially of a network of elongate plagioclase feldspar and shapeless augite masses. The diabase sheet presumably was deposited in Jurassic-Triassic time. The test cylinders were all cut with axes normal to the layering of the diabase, and parallel to the hexagonal jointing.

(V) *Vinal Haven diabase.*—The diabase obtained from Vinal Haven, Maine, is a fine- to medium-grained, very dense, dark-grayish-green rock. It is composed of essential labrodorite plagioclase and minor diopside and olivine with accessory magnetite and biotite. An approximate chemical analysis of the diabase is 48 per cent SiO_2, 18 per cent Al_2O_3, 1 per cent Fe_2O_3, 7 per cent FeO, 9 per cent MgO, 12 per cent CaO, 3 per cent Na_2O, and 0.3 per cent K_2O. The orientation of the test cylinders with respect to the geologic occurrence is not known.

Sedimentary and Metamorphic Rocks

(CS) *Cambridge slate.*—The large specimens of Cambridge slate were obtained from an abandoned quarry beside the Mystic River in Somerville, Massachusetts. The rock is called an argillite, and is a massive rock with fairly widely spaced jointing. It is late Pennsylvanian. The axes of most of the specimen cylinders were perpendicular to the bedding.

(CQ) *Cheshire quartzite.*—Several large stream bounders of the Cheshire quartzite were obtained just east of Rutland, Vermont. The quartzite is a massive, light-brown rock, somewhat pocked by weathering. It is composed of medium-grained equidimensional, interlocking quartz grains. It is a basal lower Cambrian formation. The relative attitude of cylinders and bedding is unknown.

(GS) *Green sandstone.*—The test pieces of "green sandstone" were obtained from diamond-drill cores taken in the hills to the southeast of the Catskill Mountains. The rock is an olive-gray sandstone with an argillaceous cement; it is not limy; it is a slightly indurated, medium-grained massive rock. It is from the middle Ordovician Hudson River sandstone formation. Most of the cylinders were made with axes normal to the bedding.

(RS) *Red sandstone.*—The "red sandstone" also is from the middle Ordovician Hudson River formation. It is a fine-grained, red, argillaceous sandstone; it is not limy. Test cylinders were cut from diamond-drill cores, and their axes were normal to the bedding.

(RM) *"Red marble".*—"Red marble" is the trade name for a variegated, red and white shaly limestone, imported from Italy. The contorted patterns in the fine-grained rock are distinctive. The axes of the test cylinders were all in the same direction, but their orientation to the original bedding is not known.

(SP) *Soapstone.*—The trade name of the soapstone is "Albarene stone", which is obtained from a quarry in Virginia. It is a dark-green talc schist of fine grain size. It contains about 50 per cent talc, 20 per cent chlorite, 15 per cent calcite and dolomite, 10 per cent serpentine, and 5 per cent magnetite and pyrite. Cylinder axes were perpendicular to a fairly distinct foliation.

(VA) *Verde antique.*—The name, verde antique, is applied to a decoration stone, which is mostly dark-green serpentine with white calcite streaks. The blocks were originally obtained from a quarry at Roxbury, Vermont. The quarry is in a dike of ultramafic rock originally composed of olivine and pyroxene, but altered to serpentine with some talc, calcite, brucite, hematite, amphibole, and magnetite. An approximate chemical composition of the verde antique (free of calcite) is 30 per cent SiO_2 8 per cent Fe_2O_3, 2 per cent Al_2O_3, 40 per cent MgO, 20 per cent H_2O. The axes of all test cylinders of the rock were in the same orientation, but the relationship to the attitude of the body in the quarry is unknown.

Miscellaneous Minerals

(CO) *Copper ore.*—The sulfide copper ore originally was obtained from Butte, Montana. The ore is a coarse-grained (2–5 mm) aggregate consisting predominantly of pyrite with some bornite, chalcocite, and quartz. The block of ore is massive and has no apparent foliation or lineation although there are a few vugs.

(FT) *Fluorite.*—The brown fluorite was obtained

from Clay Center, Ohio. It occurs as a massive aggregate of large (about 1-inch diameter) crystals of fluorite with some euhedral celestite crystals (½ inch long) intergrown. One hollow cylinder was made from a single crystal of purple-tinted fluorite from Cumberland, England; the axis of the cylinder was cut parallel to an a-axis.

(F) *Microline.*—A large single crystal of microcline which was originally obtained from Delaware County, Pennsylvania, was used to make up the test pieces. The crystal is closely intergrown with perthite lamellae. The test cylinders were all cut with axes parallel to the c-axis.

(P) *Pyrite.*—The pyrite specimen used for making up test pieces was obtained from Bingham, Utah. The specimen was an intergrowth of four large (about 2 inches on a side) cubic crystals of pyrite. Test cylinder axes were at odd angles to the crystals, and each cylinder included at least parts of two of the crystals.

(Q) *Quartz.*—A large single crystal of quartz which came from Brazil, was used for test specimens. The crystal has a few phantom growth planes and is considerably twinned (Dauphine). Test cylinders were cut with axes parallel both to c-axis and to an a-axis.

APPENDIX 2: DENSITY MEASUREMENTS

Rock type	Specimen type	Specimen no.	Density	Method of volume determination	Amount of perm. strain (per cent)
Solenhofen limestone	Solid cyl. (Before testing)	S-a	2.605	Micrometer measurement	
		S-b	2.600		
		S-c	2.604		
		S-d	2.597		
		Average	2.601		
Solenhofen limestone	Solid cyl. (After testing)	S-63	2.574	Micrometer measurement	2.2
		S-52	2.580		3.6
		S-68	2.577		3.0
		S-66	2.606		0.42
		S-67	2.606		0.55
Solenhofen limestone	Solid cyl. (After testing)	S-66	2.612	Water displacement	0.42
		S-67	2.610		0.55
		S-68	2.592		3.0
		S-87	2.550		8.7
		S-88	2.489		17.2
		S-90	2.506		15.1
Solenhofen limestone	Disk (After testing)	S-119	2.624	Water displacement	
		S-120	2.567		
		S-121	2.617		
Danby marble	Solid cyl. (Before testing)	DB-14B	2.702	Water displacement	
		DB-12A	2.707		
		Average	2.705		
Danby marble	Solid cyl. (After testing)	DB-11B	2.650	Water displacement	12.0
		DB-12B	2.678		8.0
Rutland White marble	Solid cyl. (Before testing)	WM-33B	2.698	Water displacement	
		WM-41A	2.691		
		Average	2.695		
Rutland White marble	Solid cyl. (After testing)	WM-23A	2.706	Water displacement	2.1
		WM-33A	2.685		7.1
		WM-41B	2.711		0.9
Wm. Henry Bay marble	Solid cyl. (Before testing)	WHB-2	2.48	Water displacement	
		WHB-3	2.61		
		Average	2.55		
Wm. Henry Bay marble	Solid cyl. (After testing)	WHB-1	2.67	Water displacement	7.2

Note: The degree of accuracy of the measurements of density is about ±.005, although given to the third place.

References Cited

Adams, F. D., and Nicolson, J. T., 1901, An experimental investigation into the flow of marble: Royal Soc. London Phil. Trans., ser. A, v. 195, p. 363–401.

—— 1910, An experimental investigation into the action of differential pressure on certain minerals and rocks, employing the process suggested by Professor Kick: Jour. Geology, v. 18, p. 489–525.

—— 1912, An experimental contribution to the question of the depth of the zone of flow in the earth's crust: Jour. Geology, v. 20, p. 97–118.

Adams, F. D., and Bancroft, J. A., 1917, Internal friction during deformation and relative plasticity of rocks: Jour. Geology, v. 25, p. 597–637.

Balsley, J. R., 1941, Deformation of marble under tension at high pressure: Am. Geophys. Union Trans., v. 22, p. 519–525.

Beliaev, N. M., and Sinitskii, A. K., 1938, Stresses and strains in thick-walled cylinders in the elastic-plastic state: Izvestia Ak. Nauk, SSSR, No. 2, p. 3–54. (Free translation by Grad. Div. App. Math., Brown Univ., 1947, for Taylor Model Basin, Contract No. bs-34166, U.S. Navy.)

Birch, F., Schairer, J. F., and Spicer, H. C. (editors), 1942, Handbook of physical constants: Geol. Soc. America Spec. Paper No. 36, 325 p.

Boeker, R., 1915, Die Mechanik der bleidbenden Formänderung in kristallinisch auf gebauten Körpern: Forschungsarbeiten V. D. I., No. 175, p. 1–51.

Bridgman, P. W., 1918, Failure of cavities in crystals and rocks under pressure: Am. Jour. Sci., 4th ser., v. 45, p. 243–268.

—— 1931, The physics of high pressures: N. Y., Macmillan Co., 398 p.

—— 1935, Effects of high shearing stress combined with high hydrostatic pressure: Phys. Rev., v. 48, p. 825–847.

—— 1936, Shearing phenomena at high pressure of possible importance for geology: Jour. Geology, v. 44, p. 653–669.

—— 1937, Shearing phenomena at high pressures, particularly in inorganic compounds: Am. Acad. Arts Sci. Proc., v. 71, p. 387–460.

—— 1939, The high pressure behavior of miscellaneous minerals: Am. Jour. Sci., v. 237, p. 7–18.

—— 1941, Explorations toward the limit of utilizable pressure: Jour. Applied Physics, v. 12, p. 461–469.

—— 1947a, Effect of hydrostatic pressure on fracture of brittle substances: Jour. Applied Physics, v. 18, p. 246–258.

—— 1947b, Fracture and hydrostatic pressure: Am. Soc. Metals Trans., v. 39, p. 246–261.

Delaney, J. P., 1940, Variation of elastic constants with moisture in soapstone: Am. Geophys. Union Trans., v. 21, p. 696–698.

Frankel, J. P., 1948, Relative strengths of portland cement mortar in bending under various loading conditions: Am. Concrete Inst. Jour., v. 20, p. 21–32.

Freudenthal, A. M., 1950, The inelastic behavior of engineering materials and structures: N. Y., John Wiley & Sons, Inc., 587 p.

Goguel, J., 1943, Introduction à l'Etude Mecanique des deformations de l'Ecorce Terrestre: Ministère Prod. Indus. et Comm. Memoir, 514 p.

Goranson, R. W., 1940, "Flow" in stressed solids: an interpretation: Geol. Soc. America Bull., v. 51, p. 1023–1034.

Griffith, A. A., 1920, The phenomena of rupture and flow in solids: Royal Soc. London Phil. Trans., ser. A, v. 221, p. 163–198.

—— 1925, The theory of rupture: 1st Internat. Cong. Applied Mechanics Proc., Delft, (1924), p. 55–63.

Griggs, D. T., 1936, Deformation of rocks under high confining pressures: Jour. Geology, v. 44, p. 541–577.

—— 1939, Creep of rocks: Jour. Geology, v. 47, p. 225–251.

—— 1940, Experimental flow of rocks under conditions favoring recrystallization: Geol. Soc. America Bull., v. 51, p. 1001–1034.

Griggs, D. T., and Miller, W. B., 1951, Deformation of Yule marble: Part I, Compression and extension experiments on dry Yule marble at 10,000 atmospheres confining pressure, room temperature: Geol Soc. America Bull., v. 62, p. 853–862.

Griggs, D. T., Turner, F. J., and Durrell, C., 1954, Deformation of Rocks at 500° C, 5000 atmospheres pressure: Geol. Soc. America Bull., v. 65, p. 1258.

Griggs, D. T., Turner, F. J., Borg, I., and Sosoka, J., 1951, Deformation of Yule marble: Part IV —Effects at 150° C: Geol. Soc. America Bull., v. 62, p. 1385–1406.

—— 1953, Deformation of Yule marble; Part IV—Effects at 300° C: Geol. Soc. America Bull., v. 64, p. 1327–1342.

Handin, J., 1953, An application of high pressure in geophysics: Experimental rock deformation: Am. Soc. Mech. Engineers Trans., v. 75, p. 315–324.

Handin, J., and Higgs, D. V., 1954, Experimental deformation of dolomite single crystals: Geol. Soc. America Bull., v. 65., p. 1263.

Jamieson, J. C., 1953, Phase equilibrium in the system calcite-aragonite: Jour. Chemical Physics, v. 21, p. 1385–1390.

Jeffreys, H., 1924, The Earth: London, Cambridge Univ. Press, 278 p.

Joffe, A. F., 1928, The physics of crystals: N. Y., McGraw-Hill Book Co., 198 p.

Jones, V., 1945, Tensile and triaxial compression tests of rock cores from the passageway to Penstock Tunnel N-4 at Boulder Dam: U.S. Bur. Reclam., Lab. Rept., No. Sp. 6, 14 p.

Karman, Th. von, 1911, Festigkeit versuche unter allseitigem Druck: Zeit. des Ver. deut. Ing., v. 55, p. 1749–1757.

King, L. V., 1912, On the limiting strength of rocks under conditions of stress existing in the earth's interior: Jour. Geology, v. 20, p. 121–126.

Love, A. E. H., 1944, A treatise on the mathematical theory of elasticity, 4th Ed.: N. Y., Dover Publ., 643 p.

Nadai, A. L., 1933, Theories of strength: Am. Soc. Mechanical Engineers Trans., v. 55, p. 123.

—— 1950, Theory of flow and fracture of solids: N. Y., McGraw Book Co., 572 p.

Orowan, E., 1940, Problems of plastic gliding: London Phys. Soc., v. 52, p. 8–22.

—— 1949, Fracture and strength of solids: London Phys. Soc., Reports on Progress in Physics, v. 12, p. 185–232.

Polanyi, M., 1921, Über die Natur des Zerreissvorganges: Zeit. Physik, v. 7, p. 323–327.

Preston, F. W., 1954, The shoe on the other foot: Am. Ceramic Soc. Bull., v. 33, p. 355–358.

Richart, F. E., Brandtzaeg, A., and Brown, R. L., 1928, A study of failure of concrete under combined compressive stresses: Univ. of Ill. Eng. Exp. Sta. Bull., No. 185, 102 p.

Weibull, W., 1939, A statistical theory of the strength of materials: Ing. Svetenskaps Acad., Hand. No. 151, 153 p.

Zwicky, F., 1923, Die Reissfestigkeit von Steinsalz: Phys. Zeit., v. 24, p. 131–137.

Dunbar Laboratory, Harvard Univ., Cambridge 38, Mass.

Manuscript Received by the Secretary of the Society March 16, 1954.

Paper No. 136 Published under the Auspices of the Committee on Experimental Geology and Geophysics and the Division of Geological Sciences at Harvard University